Published in final edited form as:
J Comp Neurol. 2009 November 10; 517(2): 226–244. doi:10.1002/cne.22158.

Ectopic Retinal ON Bipolar Cell Synapses in the OFF Inner Plexiform Layer: Contacts with Dopaminergic Amacrine Cells and Melanopsin Ganglion Cells

Olivia N. Dumitrescu[1], **Francesco G. Pucci**[1], **Kwoon Y. Wong**[1], and **David M. Berson**[2]
Department of Neuroscience, 185 Meeting Street Brown University Box G-L471 Providence, RI 02912

Abstract

A key principle of retinal organization is that distinct ON and OFF channels are relayed by separate populations of bipolar cells to different sublaminae of the inner plexiform layer (IPL). ON bipolar cell axons have been thought to synapse exclusively in the inner IPL (the ON sublamina) onto dendrites of ON-type amacrine and ganglion cells. However, M1 melanopsin-expressing ganglion cells and dopaminergic amacrine (DA) cells apparently violate this dogma. Both are driven by ON bipolar cells, but their dendrites stratify in the outermost IPL, within the OFF sublamina. Here, in the mouse retina, we show that some ON cone bipolar cells make ribbon synapses in the outermost OFF sublayer, where they costratify with and contact the dendrites of M1 and DA cells. Whole-cell recording and dye filling in retinal slices indicate that Type 6 ON cone bipolars provide some of this ectopic ON channel input. Imaging studies in dissociated bipolar cells show that these ectopic ribbon synapses are capable of vesicular release. There is thus an accessory ON sublayer in the outer IPL.

Keywords

retina; bipolar cell; ON channel circuitry; dopaminergic amacrine cell; melanopsin ganglion cell

INTRODUCTION

It has been known for decades that separate channels encoding light increments (ON) and decrements (OFF) are spawned in the outer retina and relayed to different sublaminas of the inner plexiform layer (IPL) (Famiglietti and Kolb, 1976). The ON channel is rooted in the depolarizing light responses of ON bipolar cells, reflecting sign-inverting metabotropic glutamatergic transmission from the photoreceptors (Slaughter and Miller, 1981). These ON bipolar cells, comprised of the rod bipolar cells and about half of the cone bipolar cells, have been thought to send axons exclusively to the inner three fifths of the IPL, defining its ON sublamina. Retinal ganglion cells and amacrine cells with ON-center receptive fields deploy dendrites in this sublamina, where they receive direct glutamatergic inputs from ON bipolar cell axons through ribbon synapses.

[2]To whom correspondence should be addressed. David_Berson@brown.edu.
[1]These authors contributed equally to this work.

AUTHOR CONTRIBUTIONS. O.N.D. and F.G.P. performed the immunohistochemical experiments and confocal imaging, and analyzed the histological data. K.Y.W. performed the electrophysiological recordings and FM4-64 imaging experiments, and analyzed those data. All authors wrote the paper.

The present study was prompted by an apparent violation of this tenet of retinal circuit organization by two types of inner retinal neurons: the M1 subtype of melanopsin-expressing intrinsically photosensitive retinal ganglion cells (ipRGCs) and the dopaminergic amacrine (DA) cells. Both cell types have dendrites largely or completely confined to the OFF sublayer of the IPL but receive direct excitatory drive from ON bipolar cells. Here, we sought to understand the anatomical basis of this paradoxical functional influence.

IpRGCs are novel mammalian ganglion-cell photoreceptors that mediate various reflexive responses to bright light (Berson, 2003; Fu *et al*., 2005). There is mounting evidence for multiple subclasses of melanopsin-expressing ganglion cells (Hattar *et al*., 2002; Sekaran *et al*., 2003; Tu *et al*., 2005; Dacey *et al*., 2005; Viney *et al*., 2007; Baver *et al*., 2008; Schmidt *et al*., 2008; Wong *et al*., 2008). Our focus here is on the originally described ipRGCs (Berson *et al*., 2002), which provide the dominant retinal input to the circadian pacemaker and have been termed M1 or Type 1 melanopsin cells.

The light responses of M1 cells are driven not only by intrinsic phototransduction but also by synaptic circuits originating in rods and cones. The ON channel provides the main extrinsic influence (Dacey *et al*., 2005; Perez-Leon *et al*., 2006; Wong *et al*., 2007), at least partly through direct inputs from ON bipolar cells (Wong *et al*., 2007). This is surprising because M1 cells have sparse dendritic arbors that terminate in the outermost sublamina (S1) of the IPL, within the OFF sublayer. Because most M1 cells have somas conventionally placed in the ganglion cell layer, their dendrites must ascend through the ON sublamina to reach their layer of terminal stratification in S1, so it is conceivable that ON bipolar inputs are made onto the proximal dendrites of M1 cells in the ON sublamina. Indeed, an ultrastructural survey in mouse retina found ribbon synaptic contacts onto melanopsin-immunoreactive dendrites only in the ON sublayer (Belenky *et al*., 2003; but see Jusuf *et al*., 2007). However, receptive field mapping indicates excitatory ON channel input throughout the dendritic arbor, which would encompass the OFF sublayer (Wong *et al*., 2007).

A similar paradoxical ON channel input applies to the DA cells. Light induces retinal dopamine release (Witkovsky, 2004), and this release is largely blocked by the ON channel blocker L-(+)-2-Amino-4-phosphonobutyric acid (L-AP4) (Boatright *et al*., 1994; Boelen *et al*., 1998). Electrophysiological recordings similarly showed ON light responses in many DA cells, and these are abolished in most cases by L-AP4, confirming a critical role for ON bipolar cells in this functional input. A minority of DA cells exhibit sustained ON responses that persist in the presence of L-AP4, apparently because melanopsin-based photoresponses in ipRGCs provide an excitatory drive to these cells through a circuit involving AMPA/kainate receptors (Zhang *et al*. 2007, 2008). Because the L-AP4-sensitive ON responses persist during blockade of inhibitory transmitter receptors (Zhang *et al*., 2007) or when inhibitory input is nullified by voltage-clamping at the reversal potential for chloride (Zhang *et al*. 2008), they cannot be driven by the OFF channel through a polysynaptic disinhibitory mechanism (e.g., Critz and Marc, 1992) but must be instead mediated by a direct ON bipolar cell input. It has been speculated that the necessary synaptic contacts from ON bipolar cells might occur on sparse dopaminergic processes in the ON sublayer (Witkovsky, 2004), but it is not certain that these processes belong to true dopaminergic cells, nor that they receive bipolar contacts (Kolb *et al*., 1990).

Thus, both DA and M1 cells receive a paradoxical ON channel input derived from ON bipolar cells that may be mediated in part by synapses lying outside the ON sublayer of the IPL. Because DA cells and M1 cells narrowly costratify in the outermost IPL, they may share a common source of non-canonical ON bipolar input. In cold-blooded vertebrates, bipolar cells with axon terminals in both ON and OFF sublaminas are rather common. Many of these cells are physiologically of the ON type (Pang *et al*., 2004; Wong and Dowling,

2005), so their OFF sublamina axon terminals can conceivably transmit ON channel information in the OFF IPL. By contrast, mammalian bipolar cells that are truly bistratified are very rare, though examples have been described (Famiglietti, 1981; Mariani, 1982; Kolb *et al*., 1990, 1992; Jeon and Masland, 1995; Linberg *et al*., 1996). Indeed, the giant bistratified bipolar cell first described in the primate retina has been proposed as the main source of direct ribbon synaptic input to DA cells (Hokoc and Mariani, 1987). It is not known whether these bipolar cells are functionally ON or OFF, although the giant bistratified bipolar apparently makes basal contacts with the cone pedicles, suggesting that they are probably OFF bipolars and thus may not explain the paradoxical ON channel input to DA cells. In rodents, frankly bistratified bipolar cells have not been reported, although several illustrated ON cone bipolar cells show swelling or short branches in the OFF sublayer (Ghosh *et al*., 2004; Pignatelli and Strettoi, 2004). ON bipolar cells may also make contacts in the OFF IPL in an *en passant* fashion, without overt branching. Ribbons have been observed in axonal shafts of a few ON cone bipolar cells in the outermost IPL (McGuire *et al*., 1984; Calkins *et al*., 1998), but these are atypical, and rod bipolar axons lack such ribbons (McGuire *et al*., 1984; Chun *et al*., 1993; Tsukamoto *et al*., 2001; Ghosh *et al*., 2001).

Here, we report direct anatomical evidence in the mouse that certain ON cone bipolar cells, including Type 6, make ectopic ribbon synapses in the OFF sublayer of the IPL onto the dendrites of M1 melanopsin ganglion cells and dopaminergic amacrine cells. We provide data from imaging experiments that these ribbon synapses are associated with activity-dependent cycling of synaptic vesicles. These findings suggest that the prevailing bilaminar model of ON and OFF channel segregation needs to be updated to accommodate an accessory ON sublayer in the outermost IPL.

MATERIALS AND METHODS

Animals

All procedures were in accordance with National Institutes of Health guidelines and approved by the Institutional Animal Care and Use Committee (IACUC) at Brown University. We used adult wild-type *C57Bl6* mice and three strains of genetically modified mice. In transgenic *Grm6-EGFP* mice, enhanced green fluorescent protein (EGFP) is expressed under control of the mGluR6 promoter, labeling all and only ON bipolar cells (Morgan *et al*., 2006; Dhingra *et al*., 2008). In TH::RFP mice, the tyrosine hydroxylase (TH) promoter drives the expression of red fluorescent protein, labeling all dopaminergic amacrine cells (Zhang *et al*., 2004). Finally, in *Opn4-EGFP* $^{+/-}$ mice, all melanopsin-expressing cells also express EGFP. The latter were obtained by mating homozygous knock-in *Opn4*^{Cre} animals, which express the *Cre* recombinase instead of the melanopsin (*Opn4*) open reading frame (Wong *et al*., 2008; Hattar *et al*., 2008), with the reporter line Z/EG (Jackson Laboratories). The Z/EG mouse carries a floxed beta-galactosidase/neomycin cassette and STOP sequence that can be excised by Cre-mediated recombination, triggering expression of the EGFP in Cre-expressing cells (Novak *et al*., 2000). Animals were euthanized either by carbon dioxide inhalation or by transcardial perfusion performed under deep anesthesia (ketamine HCl, 75 mg/kg, and medetomidine, 1 mg/kg, i.p.).

Electrophysiology

Whole-cell recordings were made from EGFP-labeled ipRGCs and RFP-labeled DA cells in the inner nuclear layer (INL) of isolated flat-mount retinas, and from bipolar cells in retinal slices made from wild-type or TH::RFP mice. Slices were prepared from dark-adapted animals under dim red light. Retinas were isolated from eyecups and placed photoreceptor side up on a piece of filter paper (type 0.45-μm HA; Millipore, Billerica, MA). The retina-

filter complex was held in place on a glass slide, covered with Hibernate A medium (BrainBits, Springfield IL), and cut into 300-μm slices using a custom-built chopper with Feather blades (Ted Pella, Redding, CA). The slices were incubated in bubbled Ames' medium at room temperature (RT) and kept in darkness for 10 min to 7 h before recording. Whole-cell current-clamp recordings were made from bipolar cells 3 to 5 cell layers below the slice surface using an internal solution containing (in mM) 120 K-gluconate, 5 NaCl, 4 KCl, 10 HEPES, 2 EGTA, 4 ATP-Mg, 0.3 GTP-Tris, 7 phosphocreatine-Tris, and 0.033 HyLite488-conjugated RIBEYE-binding peptide (a gift from David Zenisek, Yale University, New Haven CT; Zenisek *et al*., 2004); the pH of this solution was adjusted to 7.3 with KOH. Infrared and fluorescence images were captured with a CCD camera (CCD300T, Dage-MTI, Michigan City, IN), gated using a Dage-MTI IFG-300 image processor, and saved onto a computer using an 8-bit grayscale frame grabber card (LG-3, Scion Corporation, Frederick, MD). For flat-mount retinas, the experiments were prepared and executed as described previously (Zhang *et al*. 2008), except that QX-314 was omitted from the internal solution and that the following drugs were added to the Ringer: 300 nM tetrodotoxin (Tocris, Ellisville, MO), 5 μM strychnine (Sigma, St. Louis, MO), 20 μM bicuculline (Tocris), 10 μM (1,2,5,6-tetrahydropyridin-4-yl)methylphosphinic acid (Sigma), and 5 μM 3-[[(3,4-dichlorophenyl)methyl]amino]propyl] diethoxymethyl)phosphinic acid (Tocris). In both retinal-slice and flat-mount-retina experiments, the preparation was maintained in constant darkness except when presenting light stimuli. The light stimulus was a full-field, broadband white light with an unattenuated irradiance (i.e. −0 log I) of 2.3×10^{13} photons cm^{-2} s^{-1} sampled at 480 nm (see Wong *et al*., 2005 for the calibration method). All other electrophysiological methods and procedures were similar to those described previously in Wong *et al*. (2007).

Immunohistochemistry

Transgenic mice were transcardially perfused by pump with 30 ml of phosphate-buffered saline (PBS; 0.1 M; pH 7.4; 4°C) and immediately enucleated bilaterally. The retinas were dissected out in Ames' medium bubbled with 95% O_2, 5% CO_2 and mounted on filter paper (Millipore, HABP04700) with ganglion cells facing up. The retinas were fixed in fresh 4% paraformaldehyde (PFA) in 0.1 PBS for 30 min to 2 h, then washed in 0.1 M PBS for 1 h and cryoprotected in a sucrose solution (30% m/v in 0.2M PB; overnight at 4°C). The tissue was suspended in Optimal Cutting Temperature Compound (Ted Pella, Inc., 27050), snap frozen, and stored at −80°C. All retinas were sectioned on a Leica CM1900 cryostat and thaw-mounted on Superfrost Plus slides (Fisher Scientific, 12–550-15). Vertical sections were either 12 μm or 20 μm thick, and tangential-oblique sections were taken serially at a thickness of 5 μm. Mounted sections were incubated in blocking solution (5% normal donkey serum and 0.4% Triton X-100 in 0.1 M PBS) for 2 – 3 h at RT, then in the mixture of primary antibodies diluted in blocking solution overnight at 4°C.

Melanopsin was probed with a rabbit polyclonal antibody kindly provided by Ignacio Provencio (UF006; 1:10 000 dilution; Provencio et al., 2002). This antibody was raised against a synthetic peptide consisting of the 15 N-terminal amino acids of mouse melanopsin (MDSPSGPRVLSSLTQ). It produces no staining in melanopsin knockout mice (*Opn4* $^{-/-}$). We used one of two monoclonal antibodies raised in mouse to label presynaptic ribbons of bipolar cell axon terminals in the IPL. Synaptic ribbons were labeled with mouse monoclonal antibodies, either anti-kinesin II (Covance, MMS-198P, clone K2.4; 1:50) or anti-C-terminal binding protein 2 (CtBP2) (BD Biosciences, 612055; 1:10 000). Both antibodies produced a distinctive staining pattern of horseshoe-shaped synaptic ribbons in the OPL and dense puncta in the IPL, identical with previous reports using alternative antibodies (Muresan *et al*., 1999; Schmitz *et al*., 2000; tom Dieck *et al*., 2005). The anti-kinesin II antibody was generated against kinesin II purified from unfertilized sea urchin egg

cytosol. Anti-CtBP2 was generated using an immunogen corresponding to amino acids 361–445 of murine CtBP2, and produces the appropriate 48 kDa band in Western Blot analysis (manufacturer's data sheet). CtBP2 represents the B domain of the synaptic ribbon protein RIBEYE and its specific localization in the retina has been established previously (Schmitz *et al*., 2000). Additionally, bipolar terminals were labeled with a guinea pig polyclonal antibody against the presynaptic marker vesicular glutamate transporter 1 (vGluT1) (Millipore, AB5905; 1:10 000). This antibody was generated against a synthetic peptide from rat vGluT1 (aa 542 – 560) and produces no labeling in our tissue when preadsorbed with the immunizing antigen (Millipore, AG208). As postsynaptic markers, we used two antibodies against ionotropic glutamate receptor subunits. The first was a goat polyclonal antibody against a peptide (TNTQNYATYREGYNVYGTE) corresponding to amino acids 872–890 in the C-terminal region of human glutamate receptor 3 (GluR3; Santa Cruz Biotechnology, sc-7612; 1:100 – 1:200). Preadsorption controls with the immunizing antigen (Santa Cruz, sc-7612P) eliminated staining. The second was a rabbit polyclonal antibody raised against a synthetic peptide corresponding to amino acids 864–883 of rat glutamate receptor 2 (GluR2) and with affinity for both GluR2 and GluR3 (Millipore 07–598). This antibody detects a single band of appropriate molecular weight on Western blots of a rat brain microsomal preparation.

Other antibodies were used as well-established markers for specific retinal cell types, and in this sense their specificity for the targeted protein is immaterial. To label OFF cone bipolar cell types 1 and 2 (Haverkamp *et al*., 2003), we used a polyclonal antibody raised against neurokinin receptor 3 (NK3; 1:500; kindly provided by Arlene Hirano). The antibody was raised in rabbit against the C-terminal portion of NK3 (amino acid residues 388 – 452). Western blots from rat cortex and hypothalamus showed multiple bands from 59–83 kD m.w., and these were eliminated, as was staining in the brain, by preadsorbing the antibody with an NK3 fusion protein (Ding *et al*., 1996). We used anti-protein kinase C (PKCα) to label rod bipolar cells (Santa Cruz Biotechnology, sc-10800, 1:500 – 1:1000). This polyclonal antibody was raised in rabbit against amino acids 373 – 672 within the C-terminus of PKCα of human origin. In immunoblotting, it recognizes a single band of approximately 75 kDa in whole cell lysates of 3611-RF and NIH/3T3 cells (vendor information). Finally, we used anti-tyrosine hydroxylase (TH) to label dopaminergic amacrine cells (Millipore, AB152; 1:1000). This polyclonal antibody was raised in rabbit against denatured TH from rat pheochromocytoma. According to the vendor, a 1:1000 dilution detected TH on 10 μg of PC12 lysates.

Following the primary incubation, the tissue was washed in 0.1 M PBS for 1 h at RT and incubated again in blocking solution for 1 – 2 h. Incubation with secondary antibodies was done for 2 – 4 h at RT in the dark using AlexaFluor405 or AlexaFluor488-labeled anti-rabbit IgG raised in goat or donkey (Invitrogen, A-31556 or A-21206; 1:400) and AlexaFluor594-labeled donkey anti-mouse IgG (Invitrogen, A-21203; 1:400). Slides were washed in 0.1 M PBS for 1 h and mounted in Aqua Mount (Lerner Laboratories, 13800) or in ProLong Gold (Invitrogen, P36930).

Immunostaining was also performed on dissociated bipolar cells. Wild-type mouse retinas were dissociated as described below and plated on CC2 treated glass slides (Lab-Tek, 154852). Cell cultures were incubated in the culturing medium at 4°C for 1 h in order to allow for maximal cell adhesion. The cells were then fixed in 4% PFA in 0.1M PBS for 1 h at RT. Cells were washed twice in PBS and then incubated in blocking solution (3% normal donkey serum and 0.1% Triton X-100 in 0.1M PBS) for 1 h at RT. In order to label all ON bipolar cells, the G protein subunit Gγ13 was probed for using a rabbit polyclonal antibody (a generous gift of Robert Margolskee). This antibody was generated against amino acids 47 – 59 of mouse Gγ13 and the labeling pattern in the retina was confirmed previously by RT-

PCR and immunostaining (Huang *et al*., 2003). Primary incubation was performed overnight at 4°C using anti-Gγ13 at 1:1000 dilution in the blocking solution. Following the primary incubation, the cells were washed 3× in PBS and then incubated for 1 h at RT with AlexaFluor 488 donkey anti-rabbit IgG in the blocking solution at a dilution of 1:400. Finally, the cells were washed 3× in PBS, mounted in AquaMount, and visualized using confocal microscopy as described below.

Microscopy and image analysis

All images were obtained on a Zeiss 510 Meta inverted confocal scope equipped with Argon/2, DPSS 561–10, and Diode 405–30 lasers. For acquisition of images in tangential-oblique sections destined for quantitative and image-averaging analysis, settings and parameters were identical across all samples. For analysis involving image averaging, z-stacks consisting of 1 – 5 optical sections were acquired at depth intervals of 0.5 μm.

Images were analyzed in Zeiss LSM 510 software, Adobe Photoshop 10.0, and ImageJ. A small lateral offset of the blue channel (<0.5 μm in X and/or Y), detectable from calibration images of fluorescent beads, was corrected digitally. The laminar position of anatomical features of interest in vertical sections was recorded as a percentage of the full depth of the IPL, as inferred from the band of kinesin II-immunoreactive puncta, with 100% corresponding to the border between INL and IPL and 0% to that between the IPL and ganglion-cell layer (GCL). Synaptic ribbons were considered to be contained within ON bipolar processes only if they lay within the EGFP-positive profile in every z-plane in which they were visible.

To assess possible synapses between ON bipolar axons and M1 melanopsin or DA cell dendrites, we used an image averaging strategy closely modeled on that of Massey and colleagues (Li *et al*., 2002; Zhang *et al*., 2002). This method allows one to assess whether ectopic ON bipolar ribbons occurred in close proximity to melanopsin-positive or TH-positive dendrites at a greater-than-chance frequency. In individual images from the triple-labeled z-stacks obtained from oblique sections, we first used the immunostained plexus of M1 or TH dendrites to define the laminar zone of interest, namely, the outer part of sublamina S1. After turning off the RGB channel for the postsynaptic marker, to avoid selection bias, we identified and marked all ectopic ON bipolar ribbons within this lamina. For each such ribbon, we obtained an image sample measuring 100 pixels square and centered on the ribbon. These images were then assembled into a stack, and the average intensity of the channel for the postsynaptic marker was calculated for each pixel in the stack using the z-projection average intensity function of ImageJ. As a control for spurious signals in such image averages, we repeated the same analysis after displacing the postsynaptic marker channel by 25 μm (for melanopsin) or 100 pixels (for TH) along an axis parallel to the INL-IPL border.

The linear spacing of ectopic synapses onto melanopsin-positive or TH-positive dendrites was assessed from stacks of confocal images from 5 μm thick tangential sections of *Grm6-EGFP* retinas. We counted the ectopic contacts from ON bipolar cells onto these processes within a region of interest. The total length of immunoreactive processes was measured from the collapsed stack (z-axis projection) and divided by the total number of ectopic contacts to yield an estimate of the mean linear separation between ectopic contacts along the dendrites.

For the analysis of the stratification of recorded and dye-filled DA cells and displaced M1 cells, we generated confocal stacks encompassing the entire horizontal extent of the dendritic field, and extending, in the Z dimension, from the GCL through the full thickness of the IPL, sampled at 1 μm intervals.

Photomicrographs for this report were assembled in Adobe Photoshop 10.0. Contrast and brightness were adjusted individually for each color channel. Such manipulations were always applied globally within an image.

Dissociation of bipolar cells

Retinas were harvested, cut into halves, and digested for 45 min with 50 U/mL papain (Worthington, Lakewood NJ) either in Ringer (in mM: 135 NaCl, 3 KCl, 1 $MgCl_2$, 10 HEPES, and 10 D-glucose; pH 7.4) containing 0.5 mM $CaCl_2$ and 0.33 mg/mL cysteine, or in Hibernate A supplemented with 1.5 mM EGTA and 0.33 mg/mL cysteine. Following digestion, the retinas were rinsed 3× either with Ringer solution containing 0.2 mM $CaCl_2$ and 2 mg/mL BSA, or with Hibernate A containing 1.5 mM EGTA and 2 mg/mL BSA. The retinas were then triturated with a fire-polished Pasteur pipette in 1 mL of the same solution except that the concentration of BSA was reduced to 0.5 mg/mL. The triturated solution was placed on five HCl/ethanol-cleaned coverslips and kept at 6 °C in a refrigerator for 0.5 – 5 h prior to imaging experiments.

FM4-64 imaging

A coverslip containing dissociated bipolar cells was mounted in a chamber (Warner RC-26GLP; Hamden CT) on a fixed-stage upright microscope (Nikon E600FN; Melville NY). The cells were superfused for 2 min either with Ringer (see above) containing 2.5 mM $CaCl_2$, or with Ames' medium containing 2.5 mM $CaCl_2$. To label endocytosed synaptic vesicles, the bipolar cells were incubated for 5 – 8 min in a high-potassium solution containing 10 μM FM4-64 (Invitrogen, Carlsbad CA); this high-potassium solution was either a modified Ringer containing (in mM) 88 NaCl, 50 KCl, 1 $MgCl_2$, 2.5 $CaCl_2$, 10 HEPES, and 10 D-glucose (pH 7.4), or a mixture of 61% Ames' medium and 39% modified Ames' medium (in mM: 123.1 KCl, 0.5 KH_2PO_4, 1.24 $MgSO_4$, 4.61 $CaCl_2$, 16 D-glucose, and 22.6 $NaHCO_3$). Vesicle cycling was then halted, and FM4-64 staining in the plasma membrane was rinsed out by superfusion for 20 – 30 min with a low-calcium solution. This contained Advasep-7 (CyDex, Lenexa KS) (0.5 mM), a modified cyclodextrin scavenger for the dye, dissolved either in Ringer (see above) supplemented with 1 mM EGTA, or in Ames' medium supplemented with 2 mM EGTA. Advasep-7 was then washed out with solutions that were identical except for the omission of the scavenger. FM4-64 staining of bipolar cells was examined with a 40× water-immersion objective lens under epifluorescence using a conventional rhodamine filter set, and captured with a CCD camera (CCD300T, Dage-MTI). Fluorescence images were gated using a Dage-MTI IFG-300 image processor and saved onto a computer using an 8-bit grayscale frame grabber card (LG-3, Scion Corporation). Epifluorescence stimulus intensity and integration duration were adjusted to minimize photobleaching, optimize sensitivity and avoid saturation. To monitor vesicle release of FM4-64, bipolar cells preloaded with FM4-64 were incubated in high-potassium solutions (see above) without FM4-64 for 15 to 20 min, during which FM4-64 staining was imaged once every 5 min. To visualize synaptic ribbons within the bipolar cells, whole-cell recording was performed after FM4-64 imaging to introduce into the cells a fluorescein-conjugated version of the above-mentioned RIBEYE-binding peptide (0.033mM). The peptide was dissolved in an internal solution containing (in mM) 120 Cs-methanesulfonate, 5 NaCl, 4 CsCl, 10 HEPES, 2 EGTA, 4 ATP-Mg, 0.3 GTP-Tris, and 7 phosphocreatine-Tris, pH adjusted to 7.3 with CsOH. Peptide staining was visualized by epifluorescence using a fluorescein filter. FM4-64 fluorescence intensity was measured offline using ImageJ software.

To help distinguish ON from OFF bipolar cells, we performed immunocytochemistry on a separate group of dissociated bipolar cells using the ON bipolar cell marker G-γ13 (a gift from Robert Margolskee, Mount Sinai Medical Center, New York, NY). We measured the

length of the axons of 117 immunopositive and 113 immunonegative bipolar cells using ImageJ and the Zeiss confocal software. The axons of the immunopositive, presumed ON bipolar cells ranged from 14.1 μm to 67.4 μm, whereas the axons of immunonegative, presumed OFF bipolar cells ranged from 7.4 μm to 49.0 μm. In the FM4-64 experiment described in the previous paragraph, bipolar cells with axons ranging from 34.3 μm to 71.1 μm were analyzed; among these cells, those with axons at least 50.0 μm in length were almost certainly ON bipolar cells, whereas those shorter than 50.0 μm could be either ON or OFF.

Statistical analysis

All error estimates, including error bars in the figures, are standard errors of the mean (S.E.M.). Origin software (Microcal, Northampton MA) was used to calculate *p*-values, with the significance level set at 0.05.

RESULTS

Functional ON channel input to displaced M1 cells and DA cells in the OFF sublamina

Our initial goal was to provide a stringent test for the hypothesized ON channel input to the OFF sublayer by determining whether this input could be detected in M1 and DA cells even when they lacked any dendrites in the ON sublayer. M1 melanopsin cells with somas displaced into the INL provide an ideal test case, since their dendrites arborize in S1 but, unlike the conventionally placed M1 cells, do so without traversing the ON sublayer. To our knowledge, no recordings have been made from displaced M1 cells in any species. We made whole-cell voltage-clamp recordings of displaced M1 cells in flat-mounted retinas from *Opn4-EGFP* mice. To isolate excitatory bipolar signals, we minimized synaptic contributions from amacrine cells by setting the holding potential at E_{Cl} and by adding tetrodotoxin as well as antagonists of GABA and glycine receptors to the bath (see Methods). A 10-sec light pulse evoked an inward current with two components, as described previously (Wong *et al*., 2007): an early synaptically mediated response and a slower current generated by melanopsin-based phototransduction (Figure 1B *top*). The faster component was selectively eliminated by the ON channel blocker L-AP4 (Figure 1B *bottom*), indicating that it was generated through inputs from ON bipolar cells ($n = 3$). Intracellular filling with Lucifer Yellow confirmed that all dendrites of these M1 cells were confined to the OFF sublamina of the IPL (Figure 1A). Thus, ON bipolar cells appear to make direct excitatory synaptic contacts with the dendrites of displaced M1 cells in the OFF sublamina of the IPL.

Like displaced M1 cells, murine DA cells have somata located in the INL, so dendrites need not traverse the ON sublayer *en route* to their main arborization in S1. However, the dendritic stratification of these cells (especially those with ON channel input) has never been adequately characterized and the sparse arborization of some DA cells in the ON sublayer must be considered a possible locus of ON bipolar input (Kolb *et al*., 1990; Witkovsky, 2004; Zhang *et al*., 2007). To correlate directly the bipolar inputs and dendritic stratification of mouse DA cells, we targeted large red fluorescent protein (RFP)-positive cells in a transgenic mouse in which this protein is expressed under the control of the tyrosine hydroxylase (TH) promoter (Zhang *et al*. 2004). Under the same recording and pharmacological conditions used above to isolate bipolar inputs, all cells tested ($n = 8$) exhibited inward currents at light onset, and these were abolished by L-AP4 (Figure 1D). (Parenthetically, seven of the eight cells tested exhibited an inward current shortly after light offset, as shown in Figure 1D. This is the first direct electrophysiological demonstration, to our knowledge, of an OFF bipolar cell-driven light response in DA cells.) Dye filling of these recorded DA cells revealed that all of them were monostratified, with processes confined to the S1 layer of the OFF IPL (Figure 1C). We conclude that both DA and M1

cells receive a paradoxical ON bipolar cell input that does not involve synapses in the ON sublayer of the IPL.

Ectopic ON bipolar terminals in the OFF sublamina of the IPL

To seek anatomical support for the hypothesis that ON bipolar cells make synaptic contacts in the OFF sublayer of the IPL, we examined several retinas (n > 10) of transgenic mice (*Grm6-EGFP*) in which enhanced green fluorescent protein (EGFP) is selectively expressed in ON bipolar cells. These mice, generated by Vardi and colleagues (Morgan *et al*., 2006; Dhingra *et al*., 2008), carry an EGFP transgene driven by the promoter for metabotropic glutamate receptor 6 (mGluR6). Earlier studies of the retinas of these mice confirmed that EGFP labels all and only ON bipolar cells, including both rod bipolar cells and ON cone bipolar cells (Morgan *et al*., 2006; Dhingra *et al*., 2008). Our observations were consistent with these conclusions, in that EGFP fluorescence was limited to cells of the INL, mainly its outer two-fifths, and these cells emitted axons that followed direct descending trajectories to terminate in the inner three-fifths of the IPL, that is, within the ON sublayer (Figure 2A).

As expected from the established morphology of ON bipolar cells, EGFP-positive processes in the OFF sublamina consisted almost entirely of smooth, unbranched axonal shafts descending to their arborizations in the ON sublamina (Figure 2A). Closer examination, however, revealed clear examples of EGFP-positive swellings or boutons in the OFF sublayer (Figure 2B). Though sparsely distributed overall, they were common enough to be detectable in every section of each of the retinas examined. They usually occurred as clusters and took a variety of forms, including globular boutons, sparse axonal terminal-like arbors, and complex ring-like assemblages (Figures 2B, 3B, G–I). These terminals were similar in size to those of ON cone bipolar cell axons, which terminate mainly in the upper half of the ON sublayer, and they were smaller than the large rod bipolar terminals in the innermost IPL. Their average diameter was about 1.2 μm (n = 239).

Before concluding that these EGFP-positive terminals in the OFF sublayer derive from ON bipolar cells, it is important to consider the possibility that they result from “leaky” EGFP expression in a minority of OFF bipolar cells. We offer three lines of evidence against such a view. First, Vardi and colleagues have already shown that the EGFP expression in this mouse line is wholly coincident with immunostaining against G-γ13 (Dhingra *et al*., 2008), which is selectively expressed in ON bipolar cells (Huang *et al*., 2003). Second, the ectopic terminal-like structures could typically be traced through the z-stack to their origin in straight, smooth parent bipolar axons, which descended vertically into the ON sublayer (Figure 2B). This pattern is inconsistent with the morphology of OFF bipolar cells and suggests, instead, that the EGFP-positive terminals in the OFF sublayer constitute a secondary arborization of weakly bistratified ON bipolar cells. Finally, we tested whether immunomarkers of OFF bipolar cells might label the EGFP-positive terminals in the OFF sublayer. We used antibodies against the type 3 neurokinin receptor (NK3) to label axonal arborizations of both Type 1 and Type 2 OFF bipolar cells (Haverkamp *et al*., 2003; Ghosh *et al*., 2004). These OFF bipolar types arborize in the upper half of the OFF sublayer (i.e., layer S1), where the ectopic EGFP-positive terminals are concentrated (see below). NK3-positive and ectopic EGFP-positive terminals were intermingled in S1, but there was no colocalization (Figure 2C – E). Many of the ectopic EGFP-expressing terminals lay just above the plexus of NK3-positive axon terminals. Taken together, the evidence indicates that in the *Grm6-EGFP* mice the EGFP-positive terminals in the OFF sublayer do indeed arise from ON bipolar cells, and not from “leaky” expression of the transgene in OFF bipolar cells. In what follows, we will therefore refer to these structures as *ectopic ON bipolar terminals*.

To determine whether ectopic ON bipolar terminals might form functional output synapses, we labeled for markers of release machinery in bipolar axons. First, we visualized synaptic ribbons, a feature that, within the IPL, is restricted to bipolar terminals. We used antibodies against either kinesin II (tom Dieck *et al*., 2005) or C-terminal binding protein 2 (CtBP2) (Schmitz *et al*., 2000). As expected, both antibodies strongly labeled puncta throughout the IPL, and in the ON sublayer these were invariably localized to the EGFP-positive terminals of ON bipolar cell axons. The vast majority of ectopic ON bipolar terminals in the OFF sublamina contained at least one immunolabeled ribbon (n = 207 of 239; 87%) (Figure 3D–L, *circles*). In other experiments, we used an antibody against the type 1 vesicular glutamate transporter (vGluT1), which, within the IPL, is selectively expressed in bipolar terminals (Mimura *et al*., 2002; Haverkamp *et al*., 2003; Johnson *et al*., 2003; Sherry *et al*., 2003; Fyk-Kolodziej *et al*., 2004). This marker was clearly colocalized with EGFP in all ectopic ON bipolar terminals in the *Grm6-EGFP* mouse (Figure 3A – C). Thus, ectopic ON bipolar terminals express two proteins involved in different aspects of transmitter release machinery at bipolar terminals. We also stained for the glutamate receptor 3 subunit (GluR3), which is found postsynaptically at all bipolar cell dyads throughout the IPL (Grünert *et al*., 2002; S. Haverkamp, personal communication). Most ribbons within EGFP-positive ectopic terminals were closely coupled with GluR3 puncta (n = 54 of 87; 62%) (Figure 4A, C). We obtained similar results with the GluR2/3 antibody used by Grünert *et al*. (2002; data not shown).

En passant ON bipolar cell synapses in the OFF sublamina of the IPL

The immunolabeled ribbons in the foregoing studies were observed not only within ectopic ON bipolar boutons, but also within the smooth shafts of descending EGFP-positive axons in the OFF sublayer (Figure 3D–L, *arrowheads*). These ribbon-containing axons could be traced through the z-stack into the ON sublayer of the IPL, so there is little doubt that they arose from ON bipolar cells. The ribbons within the shafts of these axons were not associated with any obvious ectopic branching or overt bouton, although a slight local swelling of the axonal shaft was sometimes detectable. Most of these ribbons (n = 63 of 115; 55%) were also associated with postsynaptic GluR3 receptors (Figure 4A, B). They are thus likely to represent functional glutamatergic synapses of the *en passant* variety, and we will refer to them as such in this report.

Laminar distribution of ectopic ON bipolar cell synapses

Both ectopic terminals and *en passant* ribbons of ON bipolar cells appeared to be concentrated near the INL-IPL border. To assess this quantitatively, we plotted the laminar position of each ribbon-containing ectopic terminal or *en passant* synapse relative to the boundaries of the IPL, which were easily identified from the distribution of kinesin II-immunoreactive puncta. Both types of presynaptic elements were highly concentrated in the upper half of the OFF sublayer (Figure 5A), corresponding to sublamina S1. Eighty-eight percent (210 of 239) of the ectopic terminals and 63% (312 of 495) of the *en passant* ribbons of ON bipolar axons were located in S1. Density was particularly high in the outermost S1 (95–100% depth), where the dendrites of M1 cells and DA cells arborize. This laminar specificity provides indirect corroboration for our conclusion that the ribbons in the *en passant* synapses actually lie within ON bipolar axons. If they resulted instead from the occasional overlap of signals (i.e. the erroneous assignment of a ribbon within an adjacent OFF bipolar terminal to an ON bipolar shaft) they would be expected to be uniformly distributed throughout the OFF sublayer.

Spatial density and relative numbers of the two types of ectopic ON bipolar cell synapses

En passant contacts were about twice as common as ectopic terminals. For example, in a comprehensive survey of 6 vertical sections containing 722 ON bipolar ribbon synapses in

the OFF sublayer, approximately one third were contained within ectopic terminals (*n* = 227; 31%), while the remainder were *en passant* sites (*n* = 495; 69%). Within the outermost portion of S1, where they were most common, the combined density of ON bipolar cell ribbons was 1 synapse per 12 μm^2 in the plane of the whole mount retina.

Vesicular uptake and release at ectopic ON bipolar ribbon synapses

We used an imaging approach in wild-type mice to test the hypothesis that ectopic ON bipolar synapses are capable of endocytosis and release of synaptic vesicles. In primary cultures of dissociated retinal neurons, cell membranes were loaded by bath application of the styryl dye FM4-64. Dye loading was conducted in the presence of high K^+ (50 mM) and Ca^{2+} (2.5 mM) to stimulate vesicular release and endocytosis. After extensive washing to selectively eliminate dye from the plasma membrane, we scanned the axons of cells exhibiting bipolar cell morphology for evidence of fluorescent puncta indicating dye-loaded synaptic vesicles. We initially restricted the analysis to bipolar cells with axons at least 50 μm long, so as to include most ON bipolar cells but to exclude virtually all OFF bipolar cells (see Methods). As expected, all such presumed ON bipolar cells exhibited bright FM4-64 fluorescence at their most distal axonal terminals, which prior to dissociation would have occupied the ON sublayer of the IPL. In addition, however, a minority of these cells also contained fluorescent puncta at substantially more proximal locations in the axon (Figure 6). The great majority of cells had only one punctum (e.g. the two cells shown in Figure 6E), but a few had two or even three (e.g. Figure 6B). In nearly every case, these dye-positive puncta lay within the smooth, unbranched shaft of the bipolar cell axon, but very rarely they occurred within what appeared to be ectopic axonal terminals (Figure 6G–H, *arrowhead*).

To estimate the incidence of such ectopic dye-labeled puncta, we restricted consideration to the axonal segment beginning 10% of the total distance from soma to axonal terminus and ending at 80% of that distance. This was to direct the analysis, as best we could, to that part of the axon that would have traversed the OFF IPL, and to exclude segments of the axon that had probably occupied either the INL or the ON sublayer. Within this restricted intermediate stretch of the axon, 18% of the presumed ON bipolar cells examined (27 of 147) contained at least one fluorescent punctum. Nearly all of these puncta marked presumptive synapses of the *en passant* variety; only two were located in overt terminal side branches (Figure 6G – H).

In the foregoing analysis, we used a stringent criterion of minimum axonal length (50 μm), to exclude virtually all OFF bipolar cells. This stringency undoubtedly also excluded some ON bipolar cells, since these can have axons as short as 14 μm (see Methods). To determine whether ON bipolar cell types with shorter axons might also make ectopic synapses, we repeated the analysis for bipolar cells with axons 34–50 μm in length, which presumably included a mixture of ON and OFF bipolar cells. Among this group, 15% (17 of 112 cells) had ectopic fluorescent puncta within the intermediate axonal segment (i.e., 10–80% of total length), close to the same percentage observed in the more stringent ON bipolar sample. All of the presumptive synapses in this latter sample were of the *en passant* type. These data suggest that among a minority of ON bipolar cells, there is detectable vesicular cycling in the segment of their axons lying within the OFF sublayer.

To determine whether the ectopic synaptic vesicles in ON bipolar axons are capable of activity-dependent release, we stimulated a sample of the above dye-loaded presumed ON bipolar cells with solutions containing 50 mM K^+ and 2.5 mM Ca^{2+}. Most of these cells (8 of 11; 73%) showed a statistically significant and time-dependent decrease in FM4-64 intensity (25±3%, S.E.M.; $p = 0.0002$; Figure 6A – C); of these, seven had fluorescent puncta within smooth axons (*en passant* type) whereas the remaining cell had an overt ectopic terminal. The reduction in fluorescence intensity was attributable to calcium-

dependent exocytosis and not simply an artifact of dye quenching by repeated illumination. In control experiments using Ringer with low calcium and without added potassium (see Methods), repeated exposure (n = 4 to 6) to the epifluorescence light used to assess FM4-64 dye intensity did not significantly reduce the intensity measured by a single light exposure (3.8±2.4% reduction, p = 0.2; n = 4). We conclude that the reduction in FM4-64 fluorescence in ectopic synapses during superfusion with high potassium and calcium reflects the exocytosis of synaptic vesicles.

Colocalization of ectopic vesicle release sites and synaptic ribbons

Both the presence of immunolabeled synaptic ribbons in vertical sections and the cycling of synaptic vesicles in dissociated cells suggest that a minority of ON bipolar cells make functional synaptic contacts in the OFF sublayer. To determine whether these two phenomena were related, we selected a sample of isolated bipolar cells exhibiting ectopic FM4-64 axonal puncta, all of the *en passant* type. We introduced into these cells, through a patch pipette, a fluorescein-conjugated peptide that binds to synaptic ribbons with high affinity (Zenisek *et al*. 2004). In most of the cells tested (12 of 16; 75%) the ribbon-binding protein labeled puncta that clearly colocalized with the ectopic FM4-64-loaded synaptic vesicles (Figure 6D – F). The FM4-64 staining in the remaining 4 cells might indicate non-ribbon-mediated synaptic release (Zenisek 2008).

Types of ON bipolar cells making ectopic synapses in the OFF sublayer

There are at least six types of ON bipolar cells in the mouse—a single type of rod bipolar cell and five types of ON cone bipolar cells (Ghosh *et al*., 2004; Wässle et al., 2009). As a first step in determining which types of ON bipolar cells might be among those making ectopic synapses in the OFF sublayer, we selectively immunolabeled rod bipolar cells in the *Grm6-EGFP* mouse retina using an antibody against the marker protein kinase C (PKCα). None of the EGFP-positive ectopic terminals exhibited PKCα-immunoreactivity, nor did any immunolabeled rod bipolar cell show any obvious swelling or branching of its axon within the OFF sublayer of the IPL (Figure 7A, B). To assess possible *en passant* synapses in rod bipolar axons, we double immunolabeled against PKCα (for rod bipolars) and either kinesin II or CtBP2 (for ribbons). We did detect a small number of examples of apparent colocalization of ribbons within rod bipolar axonal shafts (Figure 7C). However, these were uniformly distributed throughout the full depth of the OFF sublayer, in marked contrast to the heavy concentration of all ON bipolar ribbons in the uppermost OFF sublayer (S1) (Figure 5B, compare to 5A *gray bars*). Thus, ribbons apparently localized to rod bipolar axonal shafts are certainly rare, and may simply reflect our misassignment of a nearby OFF bipolar ribbon to a rod bipolar axon. In either case, the great majority of ectopic ON bipolar ribbons appear to derive not from rod bipolar cells but rather from one or more types of ON cone bipolar cells.

In an effort to narrow down the type(s) of ON bipolar cells making ectopic synapses and to verify that these cells depolarize in response to light, we made whole-cell current-clamp recording from 61 bipolar cells in retinal slices from wild-type or TH::RFP mice. We obtained light responses from each cell and introduced the ribbon-binding fluorescent peptide into the cell through the recording pipette. Our intent was to use this peptide to locate synaptic ribbons within the cells as well as determine their morphology, but we found that the labeled ribbons, which lay at least 10 μm below the slice surface, were impossible to resolve in this material. The fluorescent peptide did, however, permit us to visualize and morphologically characterize the recorded cells. Using the morphological criteria outlined in Ghosh *et al*. (2004), 28 of the 61 recorded cells were determined to be rod bipolar cells and the rest were cone bipolars. Five of the cone bipolar cells with primary axon terminal fields in the inner IPL had lateral protrusions from the axonal shaft near the INL-IPL border.

These protrusions typically lay in the same stratum as the RFP-labeled band of DA cell processes. Two examples are shown in Figure 8A – D. All five cells had relatively compact primary axonal arbors deployed mainly in the S4 sublayer of the IPL. They thus most closely resembled Type 6 cone bipolar cells according to the criteria of Wässle et al., 2009 (see also Ghosh *et al*., 2004), although our data do not exclude their belonging instead to Type 7 or Type 8. All five of these cells generated depolarizing light responses, confirming that they were functionally ON bipolar cells (Figure 8E).

Postsynaptic targets of ectopic ON bipolar synapses in the OFF sublamina

Having established that some ON bipolar axons make functional ribbon synapses in sublamina S1, we next asked whether they make direct contact with the dendrites of M1 or DA cells, which stratify in the same sublayer. We conducted triple fluorescence studies, using the *Grm6-EGFP* mouse to visualize ON bipolar axons and two different immunofluorescent labels, one for ribbons (CtBP2 or kinesin II) and the other either for M1 cells (melanopsin) or for DA cells (TH) (Figure 9A, E).

We encountered many examples of close apposition of ectopic ON bipolar ribbons with melanopsin-positive or TH-positive dendrites in S1 (Figure 9B, C, F, G). Most of these ribbon contacts appeared to be of the *en passant* variety, although we saw examples of contacts from ectopic terminals as well. Such instances of apposition alone are not strong evidence for a functional linkage. Because both the presynaptic and postsynaptic elements under study are relatively common in S1, incidental examples of close proximity between the two would occur by chance, even if these cell types made no functional synaptic contacts. To provide a more rigorous test of such associations, we used an image averaging approach closely modeled on that introduced by Massey and colleagues (Li *et al*., 2002; Zhang *et al*., 2002). We conducted this in tangential-oblique sections because they allowed us to analyze large expanses of the S1 sublamina in single sections. With the color channel for the melanopsin signal turned off, we collected a large number of image samples (6.5 μm^2), each centered on an ectopic ON bipolar ribbon within S1. When all such images were averaged, a substantial central peak was evident in the melanopsin channel (Figure 9D, *top*). This peak was abolished in a control analysis, in which the image data for melanopsin was displaced by 25 μm before conducting the analysis (Figure 9D, *bottom*). We obtained similar results when we conducted the same sort of image averaging analysis for the DA cells (Figure 9H). Taken together, these data indicate that ectopic ON bipolar ribbons are more likely to be colocalized with M1 melanopsin dendrites or TH amacrine cell processes than would occur by chance.

Of the ectopic ON bipolar cell ribbons in S1, 44.8% (n = 104 of 232; 8 confocal stacks) were closely apposed to a melanopsin-positive dendrite, and 46.6% (n = 264 of 566; 21 confocal micrographs) showed such an association with a dopaminergic dendrite. This adds up to around 100%, but since classical bipolar terminals always form synaptic dyads within the IPL, it is difficult to say whether M1 and DA cells combined account for all postsynaptic targets of the ectopic synapses in S1. We estimate that approximately one ectopic ribbon contact is made per 54 μm of melanopsin dendrite (59 synapses in 3180.2 μm of total dendritic length, as estimated from 5 confocal micropgraphs of melanopsin-immunopositive cells). Measurements from five reconstructed M1 melanopsin cells yielded an estimate of the mean total dendritic length of 2290 μm per cell (range: 1040 – 3720 μm). Thus, each M1 melanopsin cell should receive, on average, about 42 ectopic ON bipolar ribbon synaptic inputs. We conducted the same type of analysis for the DA cells and found one ectopic ON bipolar ribbon synapse per 53 μm of TH-immunoreactive dendrite (33 synapses in 1750 μm of total dendritic length). Reconstruction of the dendritic arbors of four dye-filled DA cells resulted in an average total dendritic length of 1906 μm per cell (range: 1698 – 2276 μm).

Taken together, these findings yield an estimate of about 36 ectopic ON bipolar cell inputs per DA cell.

DISCUSSION

In this study, we have demonstrated that certain ON cone bipolar cells of the mouse retina make ribbon synaptic contacts in the OFF sublayer of the IPL. We have provided evidence that these ectopic ON bipolar presynaptic specializations are functional and are found in close contact with the dendrites of M1 melanopsin ganglion cells and dopaminergic amacrine cells at frequencies well above chance. These ectopic contacts are the most probable anatomical substrate for the paradoxical ON channel input to M1 and DA cells. More broadly, our observations suggest that the prevailing bilaminar model of ON and OFF channel segregation in the IPL should be updated to include an accessory ON sublayer in the uppermost IPL.

Caveats and alternative interpretations

Our results may be challenged on the grounds that we have placed too much faith in the *Grm6-EGFP* mouse as a means for identifying ON bipolar cells. In these mice, the reporter transgene is driven by the promoter for a metabotropic glutamate receptor (mGluR6) known to be expressed exclusively in all ON bipolar cells. While EGFP does seem to be expressed, as expected, only in ON bipolar cells (Morgan *et al*., 2006; Dhingra *et al*., 2008), reporter lines can sometimes label cells that do not actually express the driver gene. Several lines of evidence allay this concern. First, we have shown that the ectopic EGFP-positive terminals lack NK3 immunoreactivity and thus do not derive from either type of OFF bipolar cells whose arbors are concentrated in S1 of the IPL (i.e., Types 1 or 2; Ghosh *et al*., 2004). The remaining two types of OFF bipolars (Types 3 and 4) are not a plausible source of these terminals. Type 3 cells largely restrict their terminal arborization to sublayer S2 of the OFF sublamina, whereas the ectopic terminals are concentrated in S1, next to the IPL-INL border. Similarly, were the terminals derived from Type 4 cells, one would predict a broad distribution in both S1 and S2, again in conflict with the narrower observed distribution. Furthermore, we have observed side branches and boutons on the axons of physiologically identified ON bipolar cells as they pass through the OFF sublayer (Figure 8). These were observed in wild-type retina, so the phenomenon is not unique to the *Grm6-EGFP* mouse model. Regarding the ectopic *en passant* ribbons, these occur within the smooth shafts of EGFP-positive axons that pass through the OFF sublayer without branching, presumably to terminate in the ON sublayer. This arrangement cannot be explained by “leaky” expression of EGFP in OFF bipolar cells. Moreover, synaptic ribbons were observed within the smooth shafts of ON bipolar cells in culture; these were obtained from wild-type mice, again allaying any concern that this might be an idiosyncrasy of the *Grm6-EGFP* mouse.

Even if it is accepted that the cells we have studied here are ON bipolar cells, one may still challenge the inference that the ectopic axonal terminals and synaptic ribbons are indicators of functional synapses. In the case of the ectopic axon terminals in the OFF sublayer, it might be suggested that these are vestigial, a residuum from a developmental stage when the ON and OFF sublayers have not yet differentiated. The ribbons in unbranched ON bipolar axons which we suggest make *en passant* contacts in S1 might be attributed instead to the trafficking of ribbon proteins from the soma to the terminals in the ON sublayer. However, both of these objections are undercut by our observations that other components of ribbon synapses are colocalized with the ectopic ribbons in the OFF sublayer, namely, the vesicular glutamate transporter required for loading presynaptic vesicles (vGluT1) and glutamate receptor subunits (GluR3) that mediate the postsynaptic response. Further, the FM4-64 imaging data provide clear evidence of activity-dependent vesicular endocytosis and release at these ectopic sites. Also, the specialized laminar distribution of the ectopic ribbons

(mainly in upper S1) is entirely consistent with the hypothesized synaptic output to specific narrowly monostratified amacrine and ganglion cells, but is very difficult to reconcile with the ribbon trafficking hypothesis, which would predict relatively uniform distribution along these axons. Indeed, the significant colocalization of these ectopic ribbons with the dendrites of both M1 and DA cells strongly corroborates the suggestion of such specific functional contacts. Moreover, the ectopic ON bipolar axon terminals in S1 are unlikely to be a developmental anomaly of incomplete differentiation of ON and OFF bipolar cell axon terminals during development; these arbors appear to be segregated in the IPL from their first appearance, and the gradual maturation of functional ON and OFF sublayers is mainly attributable to increasing laminar precision of ganglion cell dendritic arborizations (Miller *et al*., 1999; Chalupa and Günhan, 2004). There may, however, be a developmental process of interest regarding the accessory ON sublayer. M1 ipRGCs are capable of generating intrinsic photoresponses during the differentiation of the ON and OFF sublaminas of the IPL (Hannibal and Fahrenkrug, 2004a; Sekaran *et al*., 2005; Tu *et al*., 2005). It is possible, therefore, that the accessory ON sublayer emerges from a Hebbian, activity-dependent mechanism in which ON bipolar synapses in the outer IPL are induced or stabilized by coincident depolarization of presynaptic ON bipolar terminals and postsynaptic directly photosensitive M1 cells.

Nonetheless, our central conclusion relies heavily on anatomical evidence describing synaptic sites based on coincident detection of synaptic markers in confocal images. The existence of these synapses ultimately needs confirmation from future electron microscopy studies.

A revised view of ON and OFF channel lamination in the IPL

The data presented here would seem to prompt a revision to the classic view of ON/OFF sublaminar segregation, first introduced more than 30 years ago (Famiglietti and Kolb, 1976). The revised schema would include a thin accessory ON sublayer, lying at the most distal margin of the IPL, adjacent to the INL. In contrast with the classical ON sublayer, this accessory ON sublamina appears not to be strictly segregated from the OFF sublayer. Though ON bipolar axons account for many of the ribbon synapses at the extreme distal margin of the IPL, ectopic ON bipolar terminals appear to be intermixed with those of OFF bipolar cells identified by their NK3 immunoreactivity (Figure 2C – E) or by ribbons not associated with EGFP in the *Grm6-EGFP* mouse (Figure 3D – L). It is of interest, in this context, that M1 melanopsin and DA cells, the two narrowly monostratified postsynaptic targets of the ectopic ON bipolar input, both receive weak OFF bipolar input (Figure 1D and Wong *et al*., 2007). In this sense, it may be more accurate to view the outermost IPL as a mixed ON-OFF sublayer than as purely an ON sublamina.

Identity of the ON bipolar type or types providing ectopic ON input to the OFF sublayer

There are at least six types of ON bipolar cells in the mouse retina (Ghosh et al., 2004; Wässle et al., 2009). One of these is the rod bipolar; the remaining five are cone bipolars. All of these types appear to be labeled in the *Grm6-EGFP* mouse, but only a subset of them appear to contribute ribbon synaptic inputs to the accessory ON sublayer in the distal IPL. Rod bipolar cells apparently contribute little if at all, because no ectopic terminals and very few ribbons were found in sublayer S1 within axons immunopositive for PKCα, a well established marker for murine rod bipolar cells. This is consistent with earlier reports of ribbon localization within rod bipolar cells studied immunohistochemically or by serial ultrastructural reconstruction (Chun *et al*., 1993; Tsukamoto *et al*., 2001; Ghosh *et al*., 2001), although Strettoi *et al*. (1990) noted that rod bipolar output synapses "…occasionally occurred along the axon as it coursed through the IPL." Rod signals do appear to drive M1 melanopsin cells (e.g., Dacey *et al*., 2005; Wong *et al*., 2007; see also Aggelopoulos and

Meissl, 2000), but the circuit by which they do so remains to be established. Possible circuits include the primary rod pathway involving gap junctions between AII amacrine cells and ON cone bipolar terminals, the secondary rod pathway involving rod-cone coupling, or direct contacts from rod bipolar cells to the proximal dendrites or somata of M1 cells (Ostergaard *et al*., 2007).

From the foregoing, it follows that one or more cone bipolar types are the probable source of the ectopic ON channel input to S1. In an effort to identify which of the five cone bipolar types might be responsible, we recorded and stained numerous bipolar cells in retinal slices. These studies revealed that a subset of cone bipolar cells with physiologically confirmed ON responses and primary axonal arborizations within the ON sublayer of the IPL deploy ectopic axon terminals in S1. From their relatively compact primary axonal arbors in or near S4, these cone bipolar cells appear to correspond most closely to Type 6 in the scheme of Wässle et al. (2009). However, our sample is small and lacked markers for specific IPL sublamina for reference, so it would be premature to exclude Types 7 and 8. In search of additional evidence on this point, we surveyed past descriptions and illustrations of individual bipolar cell types, marked by intracellular filling, transgenic labeling, or immunolabeling. Bipolar cells with arborizations in both the ON and OFF sublayers have been noted across a range of mammalian species, including monkey (Mariani, 1982; Rodieck, 1988), human (Kolb *et al*., 1992), cat (Famiglietti, 1981; Kolb *et al*., 1981; McGuire *et al*., 1984), rabbit (Jeon and Masland, 1995), and ground squirrel (Linberg *et al*., 1996). In rodents, however, there has been little evidence for the sort of overt terminal branches in S1 documented here. The most notable exceptions are some swellings and ectopic boutons noticeable in intracellularly stained Type 8 mouse cone bipolar cells in the study of Ghosh *et al*. (2004, Fig. 6A–C; see also a similar pattern in Pignatelli and Strettoi, 2004, Fig. 2H). In this context, it is of interest that Viney *et al*. (2007) labeled Type 8 bipolar cells in the mouse by retrograde transsynaptic transport from melanopsin-expressing ganglion cells. Note, however, that this may not reflect synaptic contacts between Type 8 bipolars and M1 melanopsin cells, since a second type of melanopsin cell (the inner-stratifying Type 2 or M2 cell) was also heavily labeled in these studies and could have been the source of the retrolabeling seen in Type 8 bipolar cells. It remains to be determined which bipolar cell types possess *en passant* synaptic ribbons. Ectopic ribbons in smooth ON bipolar axonal shafts have been detected in several ultrastructural reconstructions in cat (McGuire *et al*., 1984) and primate retina (Calkins *et al*., 1998).

Functional considerations

The impetus for this study was the need to identify the anatomical substrate for ON channel input to two types of retinal neurons whose dendrites arborized in the OFF sublamina of the IPL: the M1 melanopsin ipRGCs and the DA cells. We have provided evidence for sparse ON bipolar inputs to the dendrites of these cells in the OFF sublayer. Are these inputs sufficient to account for the observed ON responses of these cells? We estimate that there are on average a total of roughly 40 ectopic ON bipolar contacts onto each DA and M1 melanopsin cell. The estimate for M1 cells is reasonably close to the findings of Jusuf *et al*. (2007), who reported that M1-like, outer-stratifying melanopsin cells in the marmoset receive, on average, just over a hundred ribbon synaptic contacts in the outer (OFF) IPL; that study did not determine whether these contacts came from ON or OFF bipolar cells. The total numbers of bipolar inputs to ganglion cells cover a remarkably broad range across various cell types and species, ranging from about a dozen to many thousands (Kolb and Dekorver, 1991; Freed *et al*., 1992; Jusuf *et al*., 2007; Eriköz *et al*., 2008; Xu *et al*., 2008). M1 cells fall within this range, albeit at its lower end. Two ganglion cell types have total bipolar ribbon contacts that are at least this low (Ghosh and Grünert, 1999; Eriköz *et al*., 2008), although both types have much smaller dendritic fields than the M1 cells. Before a

strong case can be made that a few dozen ribbon contacts are sufficient to account for the observed light-evoked excitatory currents in these cells, more needs to be learned about the size of synaptic currents generated by individual bipolar contacts onto M1 cells and about the passive and active spread of such currents through the M1 dendritic arbor.

At least for the DA cells and displaced M1 cells we recorded and stained, both of which lack processes in the main ON sublayer, it is unclear what circuit other than that proposed here could account for the physiological ON responses, given that these require glutamatergic transmission and persist when inhibition is blocked. For conventionally placed M1 cells, an alternative locus of ON bipolar input is onto their proximal dendrites as they traverse the ON sublayer. Ribbon contacts onto melanopsin-immunoreactive processes in the ON sublayer have been observed ultrastructurally (Belenky *et al*., 2003), but it has not been excluded that the postsynaptic elements are the dendrites of M2 cells (which arborize in the ON sublayer), rather than of M1 cells. With respect to the DA cells, there is evidence for sparse tyrosine hydroxylase immunoreactive processes in the ON sublayer (Kolb *et al*., 1990; Witkovsky, 2004; Zhang *et al*., 2007), so at least some DA cells may receive ON channel input in the ON sublayer in addition to, or instead of, in the OFF sublayer.

It will be of interest to learn whether ON signals transmitted in the accessory ON sublayer differ functionally from those in the main ON sublayer. Such differences could arise if the type(s) of cone bipolar cells synapsing in this accessory ON sublayer have distinctive functional features. In addition, there might be substantial functional differences in the amacrine inhibitory influences on bipolar-to-ganglion-cell transmission in this sublayer. For example, if local tonic amacrine cell inhibition were driven mainly by the OFF channel rather than the ON channel, this might shield the ectopic ON bipolar synapses from sustained ON inhibition. Such inhibition has been shown to truncate ON responses passing through the ON sublayer (Roska *et al*., 1998), so the ON bipolar drive to postsynaptic targets may be relatively more sustained in the accessory ON sublayer than it is in the classical ON sublayer. It is therefore of interest that the ON channel excitatory synaptic drive to the ipRGCs is substantially more sustained than it is in other ON ganglion cells (Wong *et al*., 2007).

Supplementary Material

Refer to Web version on PubMed Central for supplementary material.

Acknowledgments

We are very grateful to Noga Vardi for generously providing the *Grm6-EGFP* transgenic mice, to Doug McMahon for the TH::RFP mice, and to Samer Hattar and Jen Ecker for the invaluable $Opn4^{Cre}$ mice. We also thank Stephen Massey for advice on, and custom software for, image-averaging analysis of confocal micrographs. We are grateful to David Zenisek for the RIBEYE-binding fluorescent peptide, Arlene Hirano for providing the anti-NK3 antibody and Robert Margolskee for the anti-G γ13 antibody. Marie Fina and Dianne Boghossian provided excellent technical assistance with the preparation of some of the retinas.

Grant sponsor: NIH. Grant numbers: K99 EY18863 (to K.Y.W.) and R01 EY012793 (to D.M.B.)

LITERATURE CITED

Aggelopoulos NC, Meissl H. Responses of neurones of the rat suprachiasmatic nucleus to retinal illumination under photopic and scotopic conditions. J Physiol. 2000; 523(Pt 1):211–222. [PubMed: 10673556]

Baver SB, Pickard GE, Sollars PJ. Two types of melanopsin retinal ganglion cell differentially innervate the hypothalamic suprachiasmatic nucleus and the olivary pretectal nucleus. Eur J Neurosci. 2008; 27(7):1763–1770. [PubMed: 18371076]

Belenky MA, Smeraski CA, Provencio I, Sollars PJ, Pickard GE. Melanopsin retinal ganglion cells receive bipolar and amacrine cell synapses. J Comp Neurol. 2003; 460(3):380–393. [PubMed: 12692856]

Berson DM. Strange vision: ganglion cells as circadian photoreceptors. Trends Neurosci. 2003; 26(6): 314–320. [PubMed: 12798601]

Berson DM, Dunn FA, Takao M. Phototransduction by retinal ganglion cells that set the circadian clock. Science. 2002; 295(5557):1070–1073. [PubMed: 11834835]

Boatright JH, Gordon JR, Iuvone PM. Inhibition of endogenous dopamine release in amphibian retina by L-2-amino-4-phosphonobutyric acid (L-AP4) and trans-2-aminocyclopentane-1,3-dicarboxylate (ACPD). Brain Res. 1994; 649(1–2):339–342. [PubMed: 7525012]

Boelen MK, Boelen MG, Marshak DW. Light-stimulated release of dopamine from the primate retina is blocked by 1-2-amino-4-phosphonobutyric acid (APB). Vis Neurosci. 1998; 15(1):97–103. [PubMed: 9456509]

Calkins DJ, Tsukamoto Y, Sterling P. Microcircuitry and mosaic of a blue-yellow ganglion cell in the primate retina. J Neurosci. 1998; 18(9):3373–3385. [PubMed: 9547245]

Chalupa LM, Gunhan E. Development of On and Off retinal pathways and retinogeniculate projections. Prog Retin Eye Res. 2004; 23(1):31–51. [PubMed: 14766316]

Chun MH, Han SH, Chung JW, Wässle H. Electron microscopic analysis of the rod pathway of the rat retina. J Comp Neurol. 1993; 332(4):421–432. [PubMed: 8349841]

Critz SD, Marc RE. Glutamate antagonists that block hyperpolarizing bipolar cells increase the release of dopamine from turtle retina. Vis Neurosci. 1992; 9(3–4):271–278. [PubMed: 1327088]

Dacey DM, Liao HW, Peterson BB, Robinson FR, Smith VC, Pokorny J, Yau KW, Gamlin PD. Melanopsin-expressing ganglion cells in primate retina signal colour and irradiance and project to the LGN. Nature. 2005; 433(7027):749–754. [PubMed: 15716953]

Dhingra A, Sulaiman P, Xu Y, Fina ME, Veh RW, Vardi N. Probing neurochemical structure and function of retinal ON bipolar cells with a transgenic mouse. J Comp Neurol. 2008; 510(5):484–496. [PubMed: 18671302]

Ding YQ, Shigemoto R, Takada M, Ohishi H, Nakanishi S, Mizuno N. Localization of the neuromedin K receptor (NK3) in the central nervous system of the rat. J Comp Neurol. 1996; 364:290–310. [PubMed: 8788251]

Erikoz B, Jusuf PR, Percival KA, Grunert U. Distribution of bipolar input to midget and parasol ganglion cells in marmoset retina. Vis Neurosci. 2008; 25(1):67–76. [PubMed: 18282311]

Famiglietti EV Jr. Functional architecture of cone bipolar cells in mammalian retina. Vision Res. 1981; 21(11):1559–1563. [PubMed: 7336584]

Famiglietti EV Jr, Kolb H. Structural basis for ON-and OFF-center responses in retinal ganglion cells. Science. 1976; 194(4261):193–195. [PubMed: 959847]

Freed MA, Smith RG, Sterling P. Computational model of the on-alpha ganglion cell receptive field based on bipolar cell circuitry. Proc Natl Acad Sci U S A. 1992; 89(1):236–240. [PubMed: 1309606]

Fu Y, Liao HW, Do MT, Yau KW. Non-image-forming ocular photoreception in vertebrates. Curr Opin Neurobiol. 2005; 15(4):415–422. [PubMed: 16023851]

Fyk-Kolodziej B, Dzhagaryan A, Qin P, Pourcho RG. Immunocytochemical localization of three vesicular glutamate transporters in the cat retina. J Comp Neurol. 2004; 475(4):518–530. [PubMed: 15236233]

Ghosh KK, Bujan S, Haverkamp S, Feigenspan A, Wässle H. Types of bipolar cells in the mouse retina. J Comp Neurol. 2004; 469(1):70–82. [PubMed: 14689473]

Ghosh KK, Grunert U. Synaptic input to small bistratified (blue-ON) ganglion cells in the retina of a new world monkey, the marmoset Callithrix jacchus. J Comp Neurol. 1999; 413(3):417–428. [PubMed: 10502249]

Ghosh KK, Haverkamp S, Wässle H. Glutamate receptors in the rod pathway of the mammalian retina. J Neurosci. 2001; 21(21):8636–8647. [PubMed: 11606651]

Grunert U, Haverkamp S, Fletcher EL, Wässle H. Synaptic distribution of ionotropic glutamate receptors in the inner plexiform layer of the primate retina. J Comp Neurol. 2002; 447(2):138–151. [PubMed: 11977117]

Hannibal J, Fahrenkrug J. Melanopsin containing retinal ganglion cells are light responsive from birth. Neuroreport. 2004; 15(15):2317–2320. [PubMed: 15640747]

Hattar, S.; Ecker, JL.; Dumitrescu, ON.; Wong, KY.; Berson, DM. Neuroscience. Washington D.C: 2008. Melanopsin cells comprise an anatomically and functionally distinct population of retinal ganglion cells in the mouse. Abstract in Society for.

Hattar S, Liao HW, Takao M, Berson DM, Yau KW. Melanopsin-containing retinal ganglion cells: architecture, projections, and intrinsic photosensitivity. Science. 2002; 295(5557):1065–1070. [PubMed: 11834834]

Haverkamp S, Ghosh KK, Hirano AA, Wässle H. Immunocytochemical description of five bipolar cell types of the mouse retina. J Comp Neurol. 2003; 455(4):463–476. [PubMed: 12508320]

Hokoc JN, Mariani AP. Tyrosine hydroxylase immunoreactivity in the rhesus monkey retina reveals synapses from bipolar cells to dopaminergic amacrine cells. J Neurosci. 1987; 7(9):2785–2793. [PubMed: 2887643]

Huang L, Max M, Margolskee RF, Su H, Masland RH, Euler T. G protein subunit G gamma 13 is coexpressed with G alpha o, G beta 3, and G beta 4 in retinal ON bipolar cells. J Comp Neurol. 2003; 455(1):1–10. [PubMed: 12454992]

Jeon CJ, Masland RH. A population of wide-field bipolar cells in the rabbit's retina. J Comp Neurol. 1995; 360(3):403–412. [PubMed: 8543648]

Johnson J, Tian N, Caywood MS, Reimer RJ, Edwards RH, Copenhagen DR. Vesicular neurotransmitter transporter expression in developing postnatal rodent retina: GABA and glycine precede glutamate. J Neurosci. 2003; 23(2):518–529. [PubMed: 12533612]

Jusuf PR, Lee SC, Hannibal J, Grunert U. Characterization and synaptic connectivity of melanopsin-containing ganglion cells in the primate retina. Eur J Neurosci. 2007; 26(10):2906–2921. [PubMed: 18001286]

Kolb H, Cuenca N, Wang HH, Dekorver L. The synaptic organization of the dopaminergic amacrine cell in the cat retina. J Neurocytol. 1990; 19(3):343–366. [PubMed: 2391538]

Kolb H, Dekorver L. Midget ganglion cells of the parafovea of the human retina: a study by electron microscopy and serial section reconstructions. J Comp Neurol. 1991; 303(4):617–636. [PubMed: 1707423]

Kolb H, Linberg KA, Fisher SK. Neurons of the human retina: a Golgi study. J Comp Neurol. 1992; 318(2):147–187. [PubMed: 1374766]

Kolb H, Nelson R, Mariani A. Amacrine cells, bipolar cells and ganglion cells of the cat retina: a Golgi study. Vision Res. 1981; 21(7):1081–1114. [PubMed: 7314489]

Li W, Trexler EB, Massey SC. Glutamate receptors at rod bipolar ribbon synapses in the rabbit retina. J Comp Neurol. 2002; 448(3):230–248. [PubMed: 12115706]

Linberg KA, Suemune S, Fisher SK. Retinal neurons of the California ground squirrel, Spermophilus beecheyi: a Golgi study. J Comp Neurol. 1996; 365(2):173–216. [PubMed: 8822165]

Mariani AP. Biplexiform cells: ganglion cells of the primate retina that contact photoreceptors. Science. 1982; 216(4550):1134–1136. [PubMed: 6177044]

McGuire BA, Stevens JK, Sterling P. Microcircuitry of bipolar cells in cat retina. J Neurosci. 1984; 4(12):2920–2938. [PubMed: 6502212]

Miller ED, Tran MN, Wong GK, Oakley DM, Wong RO. Morphological differentiation of bipolar cells in the ferret retina. Vis Neurosci. 1999; 16(6):1133–1144. [PubMed: 10614593]

Mimura Y, Mogi K, Kawano M, Fukui Y, Takeda J, Nogami H, Hisano S. Differential expression of two distinct vesicular glutamate transporters in the rat retina. Neuroreport. 2002; 13(15):1925–1928. [PubMed: 12395093]

Morgan JL, Dhingra A, Vardi N, Wong RO. Axons and dendrites originate from neuroepithelial-like processes of retinal bipolar cells. Nat Neurosci. 2006; 9(1):85–92. [PubMed: 16341211]

Muresan V, Lyass A, Schnapp BJ. The kinesin motor KIF3A is a component of the presynaptic ribbon in vertebrate photoreceptors. J Neurosci. 1999; 19(3):1027–1037. [PubMed: 9920666]

Novak A, Guo C, Yang W, Nagy A, Lobe CG. Z/EG, a double reporter mouse line that expresses enhanced green fluorescent protein upon Cre-mediated excision. Genesis. 2000; 28:147–155. [PubMed: 11105057]

Ostergaard J, Hannibal J, Fahrenkrug J. Synaptic contact between melanopsin-containing retinal ganglion cells and rod bipolar cells. Invest Ophthalmol Vis Sci. 2007; 48(8):3812–3820. [PubMed: 17652756]

Pang JJ, Gao F, Wu SM. Stratum-by-stratum projection of light response attributes by retinal bipolar cells of Ambystoma. J Physiol. 2004; 558(Pt 1):249–262. [PubMed: 15146053]

Perez-Leon JA, Warren EJ, Allen CN, Robinson DW, Lane Brown R. Synaptic inputs to retinal ganglion cells that set the circadian clock. Eur J Neurosci. 2006; 24(4):1117–1123. [PubMed: 16930437]

Pignatelli V, Strettoi E. Bipolar cells of the mouse retina: a gene gun, morphological study. J Comp Neurol. 2004; 476(3):254–266. [PubMed: 15269969]

Provencio I, Rollag MD, Castrucci AM. Photoreceptive net in the mammalian retina. Nature. 2002; 415(6871):493. [PubMed: 11823848]

Rodieck, RW. The primate retina. In: Steklis, HD., editor. Comparative Primate Biology. New York: Alan R. Liss; 1988. p. 203-278.

Roska B, Nemeth E, Werblin FS. Response to change is facilitated by a three-neuron disinhibitory pathway in the tiger salamander retina. J Neurosci. 1998; 18(9):3451–3459. [PubMed: 9547252]

Schmidt TM, Taniguchi K, Kofuji P. Intrinsic and extrinsic light responses in melanopsin-expressing ganglion cells during mouse development. J Neurophysiol. 2008; 100(1):371–384. [PubMed: 18480363]

Schmitz F, Konigstorfer A, Sudhof TC. RIBEYE, a component of synaptic ribbons: a protein's journey through evolution provides insight into synaptic ribbon function. Neuron. 2000; 28(3):857–872. [PubMed: 11163272]

Sekaran S, Foster RG, Lucas RJ, Hankins MW. Calcium imaging reveals a network of intrinsically light-sensitive inner-retinal neurons. Curr Biol. 2003; 13(15):1290–1298. [PubMed: 12906788]

Sekaran S, Lupi D, Jones SL, Sheely CJ, Hattar S, Yau KW, Lucas RJ, Foster RG, Hankins MW. Melanopsin-dependent photoreception provides earliest light detection in the mammalian retina. Curr Biol. 2005; 15(12):1099–1107. [PubMed: 15964274]

Sherry DM, Wang MM, Bates J, Frishman LJ. Expression of vesicular glutamate transporter 1 in the mouse retina reveals temporal ordering in development of rod vs. cone and ON vs. OFF circuits. J Comp Neurol. 2003; 465(4):480–498. [PubMed: 12975811]

Slaughter MM, Miller RF. 2-amino-4-phosphonobutyric acid: a new pharmacological tool for retina research. Science. 1981; 211(4478):182–185. [PubMed: 6255566]

Strettoi E, Dacheux RF, Raviola E. Synaptic connections of rod bipolar cells in the inner plexiform layer of the rabbit retina. J Comp Neurol. 1990; 295(3):449–466. [PubMed: 2351763]

tom Dieck S, Altrock WD, Kessels MM, Qualmann B, Regus H, Brauner D, Fejtova A, Bracko O, Gundelfinger ED, Brandstatter JH. Molecular dissection of the photoreceptor ribbon synapse: physical interaction of Bassoon and RIBEYE is essential for the assembly of the ribbon complex. J Cell Biol. 2005; 168(5):825–836. [PubMed: 15728193]

Tsukamoto Y, Morigiwa K, Ueda M, Sterling P. Microcircuits for night vision in mouse retina. J Neurosci. 2001; 21(21):8616–8623. [PubMed: 11606649]

Tu DC, Zhang D, Demas J, Slutsky EB, Provencio I, Holy TE, Van Gelder RN. Physiologic diversity and development of intrinsically photosensitive retinal ganglion cells. Neuron. 2005; 48(6):987–999. [PubMed: 16364902]

Viney TJ, Balint K, Hillier D, Siegert S, Boldogkoi Z, Enquist LW, Meister M, Cepko CL, Roska B. Local retinal circuits of melanopsin-containing ganglion cells identified by transsynaptic viral tracing. Curr Biol. 2007; 17(11):981–988. [PubMed: 17524644]

Wässle H, Puller C, Müller F, Haverkamp S. Cone contacts, mosaics, and territories of bipolar cells in the mouse retina. J Neurosci. 2009; 29(1):106–117. [PubMed: 19129389]

Witkovsky P. Dopamine and retinal function. Doc Ophthalmol. 2004; 108(1):17–40. [PubMed: 15104164]

Wong KY, Dowling JE. Retinal bipolar cell input mechanisms in giant danio. III. ON-OFF bipolar cells and their color-opponent mechanisms. J Neurophysiol. 2005; 94(1):265–272. [PubMed: 15758056]

Wong KY, Dunn FA, Berson DM. Photoreceptor adaptation in intrinsically photosensitive retinal ganglion cells. Neuron. 2005; 48(6):1001–1010. [PubMed: 16364903]

Wong KY, Dunn FA, Graham DM, Berson DM. Synaptic influences on rat ganglion-cell photoreceptors. J Physiol. 2007; 582(Pt 1):279–296. [PubMed: 17510182]

Wong, KY.; Ecker, JL.; Dumitrescu, ON.; Berson, DM.; Hattar, S. Abstract in Association for Research in Vision and Ophthalmology. Ft. Lauderdale: 2008. Multiple Morphological Types of Melanopsin Ganglion Cells with Distinct Light Responses and Axonal Targets.

Xu Y, Vasudeva V, Vardi N, Sterling P, Freed MA. Different types of ganglion cell share a synaptic pattern. J Comp Neurol. 2008; 507(6):1871–1878. [PubMed: 18271025]

Zenisek D. Vesicle association and exocytosis at ribbon and extraribbon sites in retinal bipolar cell presynaptic terminals. Proc Natl Acad Sci U S A. 2008; 105(12):4922–4927. [PubMed: 18339810]

Zenisek D, Horst NK, Merrifield C, Sterling P, Matthews G. Visualizing synaptic ribbons in the living cell. J Neurosci. 2004; 24(44):9752–9759. [PubMed: 15525760]

Zhang DQ, Stone JF, Zhou T, Ohta H, McMahon DG. Characterization of genetically labeled catecholamine neurons in the mouse retina. Neuroreport. 2004; 15(11):1761–1765. [PubMed: 15257143]

Zhang DQ, Wong KY, Sollars PJ, Berson DM, Pickard GE, McMahon DG. Intraretinal signaling by ganglion cell photoreceptors to dopaminergic amacrine neurons. Proc Natl Acad Sci U S A. 2008; 105(37):14181–14186. [PubMed: 18779590]

Zhang DQ, Zhou TR, McMahon DG. Functional heterogeneity of retinal dopaminergic neurons underlying their multiple roles in vision. J Neurosci. 2007; 27(3):692–699. [PubMed: 17234601]

Zhang J, Li W, Trexler EB, Massey SC. Confocal analysis of reciprocal feedback at rod bipolar terminals in the rabbit retina. J Neurosci. 2002; 22(24):10871–10882. [PubMed: 12486181]

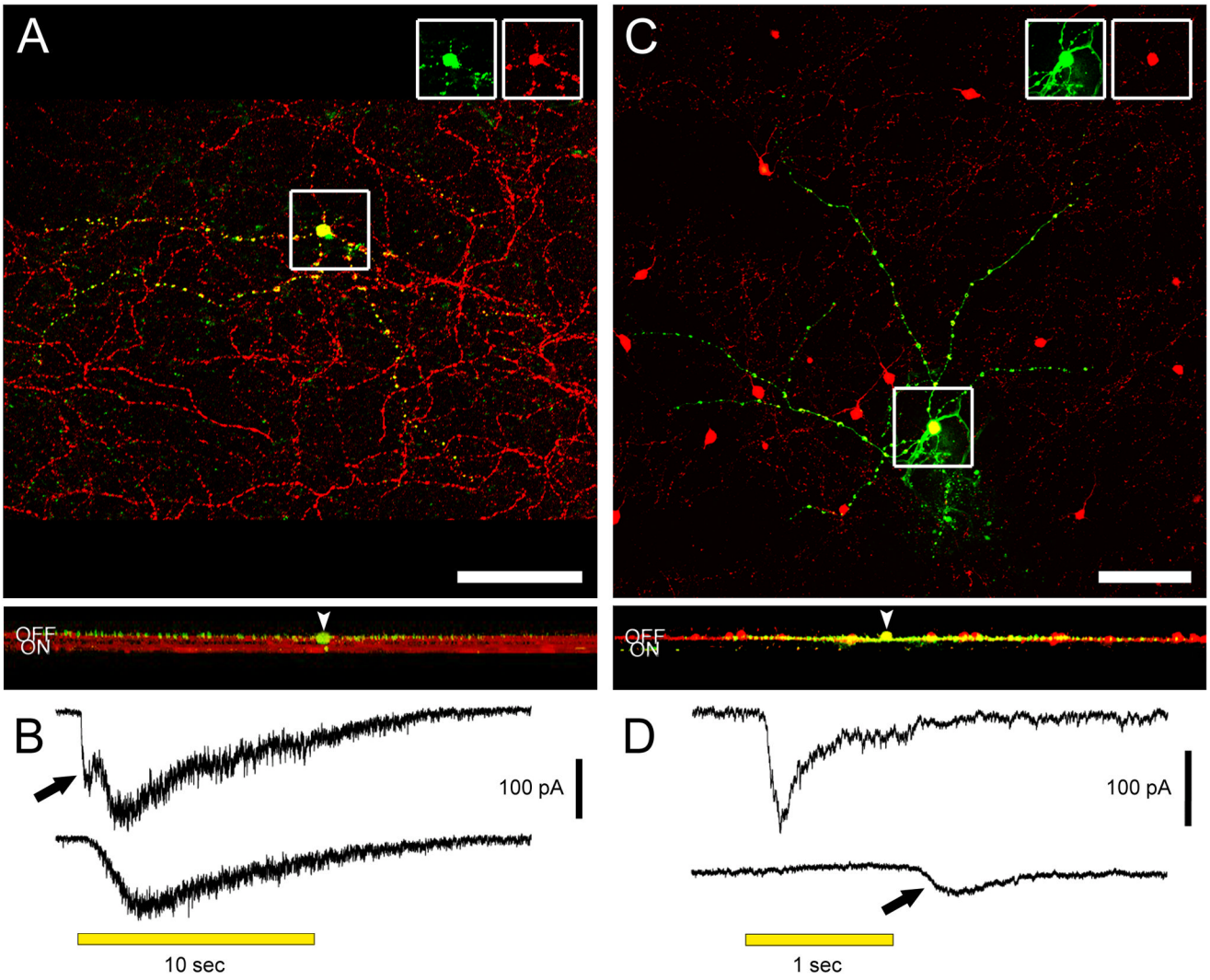

Figure 1. M1 intrinsically photosensitive ganglion cells and dopaminergic amacrine (DA) cells stratify in the OFF sublamina of the IPL, but receive physiological ON channel excitatory inputs

A. A displaced M1 cell filled with Lucifer Yellow (*green*) during whole-cell recording and later immunostained against melanopsin (*red*). *Top panel* shows the recorded cell and the plexus of melanopsin-positive M1 dendrites in a confocal stack projection of the outer IPL as seen in the whole-mount. Insets at top separate the signals and confirm that the Lucifer Yellow-filled cell expressed melanopsin. Scale bar 100 μm. *Bottom panel* is a virtual vertical view obtained by 90 degree x-axis rotation and projection of the entire confocal stack. Two bands can be seen in the red channel, corresponding to the level of dendritic stratification levels of M1 cells (upper band; OFF sublamina) and M2 cells (lower band; ON sublamina). Note that all dendrites of the filled M1 cell are restricted to the OFF sublamina. *Arrowhead* points to the cell body, displaced to the INL. **B**. Voltage-clamp recordings from the displaced M1 cell in *A* revealing an ON bipolar cell-driven light response. The recordings were made under conditions that minimized amacrine cell input (see text). *Top trace:* The control light response consisted of a fast inward current (*arrow*) that was followed by a slower one. *Bottom trace:* L-AP4 selectively eliminated the fast component, indicating its generation by ON bipolar cells. **C**. A dopaminergic amacrine cell expressing RFP (*red;* TH::RFP retina) and filled with Alexa488 (*green*) during whole-cell recording.

Top panel shows the cell in the whole-mount view, in the collapsed confocal stack. Insets as for *A*. Scale bar 100 μm. *Bottom panel* shows the projected x-axis rotation of the same confocal stack, imaged from the GCL throughout the INL. The red RFP band corresponds to the main dendritic plexus of the dopaminergic cells (outer OFF sublamina). All processes of the filled DA cell are restricted to this sublamina. Very faint green specks lower in the IPL are histological artifacts not traceable to the dye-filled cell. *Arrowhead* indicates the cell body in the INL. A magenta-green version of the photomicrographs in this figure is available online as a supplemental figure. **D**. Voltage-clamp recordings from the DA cell in *C* demonstrating an ON bipolar-mediated light response. *Top trace:* Under conditions that minimized inhibitory input (see text), an inward current was observed at light onset. *Bottom trace:* Application of L-AP4 abolished the inward current at light onset, confirming that it was mediated by ON bipolar cells. In addition, a smaller inward current at light off appeared (*arrow*), which presumably reflects an input from OFF bipolar cells. All light stimuli were −1 log I.

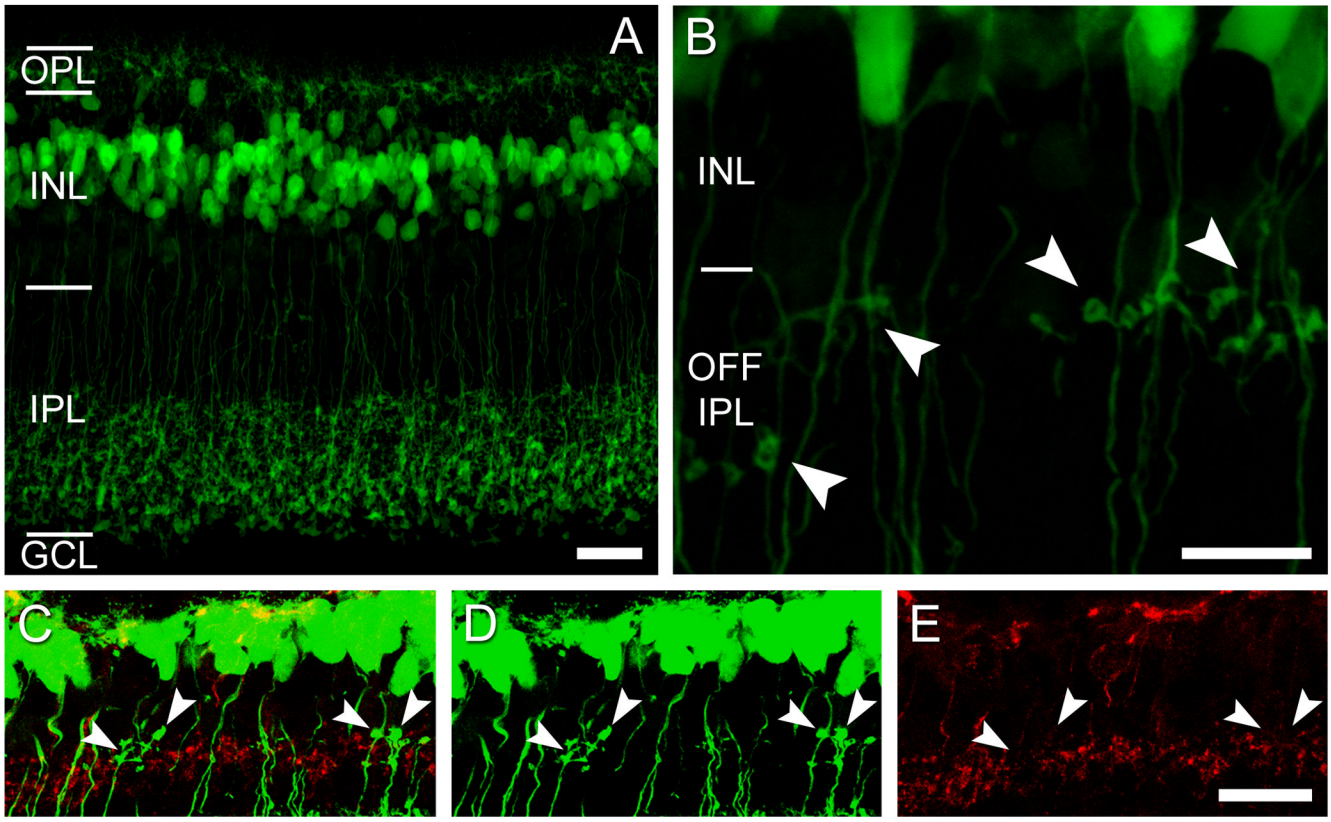

Figure 2. ON bipolar cell axons deploy ectopic terminals in the OFF IPL

A. Vertical section of a *Grm6-EGFP* retina, showing strong expression of the fluorescent reporter (*green*) in all and only ON bipolar cells, including their axon terminals in the lower three fifths of the INL (ON sublayer). Scale bar 20 μm. **B**. Higher magnification in the OFF sublamina of the IPL, showing lateral terminal-like structures arising from EGFP-positive ON bipolar cell axons. Note that in most cases the primary axons can be followed to further descend into the inner IPL. Scale bar 10 μm. **C – E**. *Grm6-EGFP* retina immunostained for NK3 (*red*), a marker of Types 1 and 2 OFF cone bipolar cells, known to terminate in the upper half of the OFF sublayer. *C* shows the merged image; *D* the EGFP and *E* the NK3 alone. *Arrowheads* indicate EGFP-positive ectopic ON bipolar terminals, which intermingle but never colocalize with NK3-positive OFF bipolar terminals. Scale bar 20 μm. All panels are projected confocal stacks. A magenta-green version of this figure is available online as a supplemental figure.

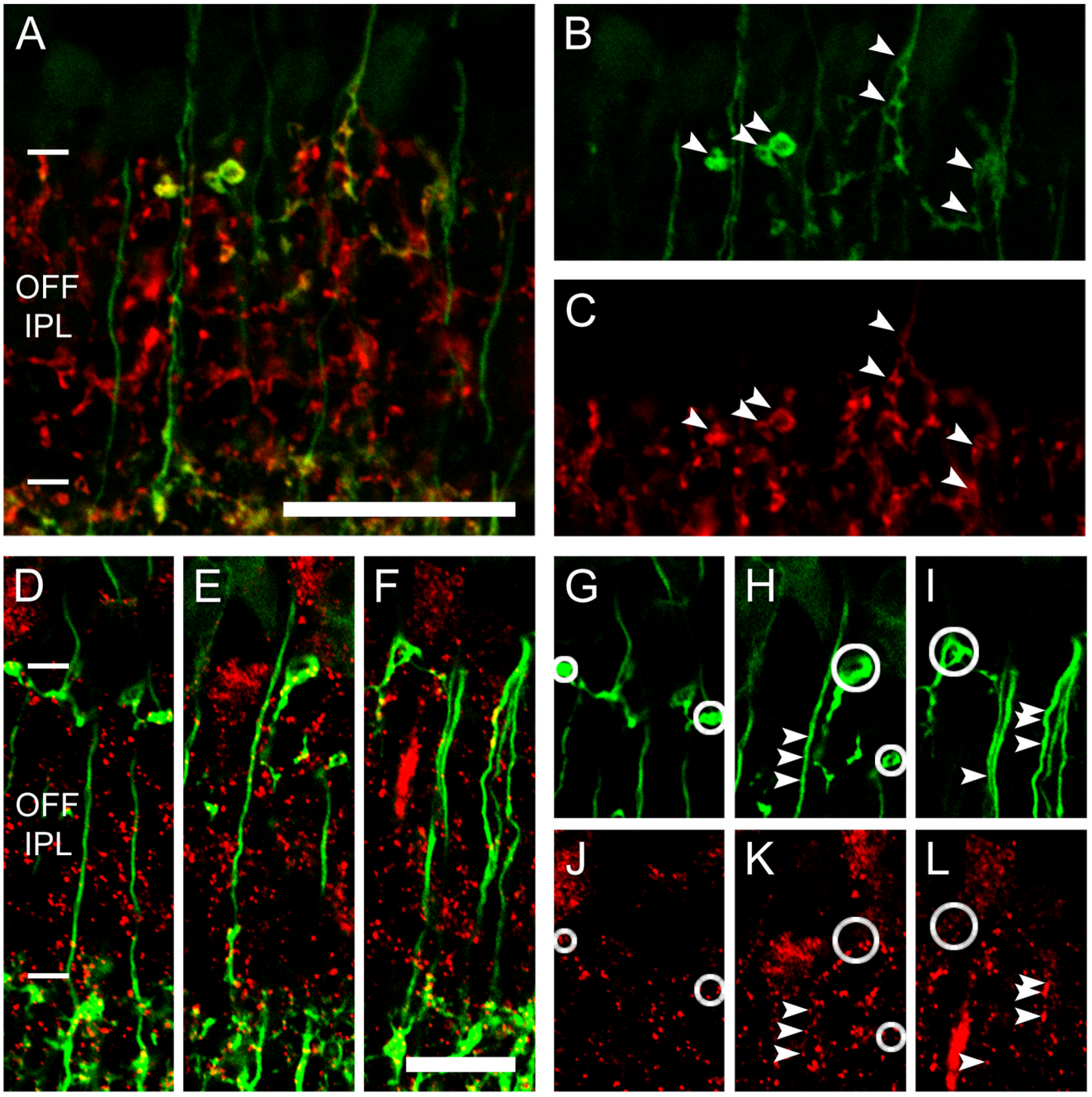

Figure 3. The ectopic ON bipolar cell terminals in the OFF IPL express presynaptic markers

A. Image of the OFF IPL in a vertical section of *Grm6-EGFP* retina immunostained for vGluT1 (*red*). Single confocal plane. Scale bar 20 μm. **B – C**. Split channels of the same image as in *A*, with *arrowheads* pointing to all EGFP ectopic terminals (*green)*, which always colocalize with the vGluT1 labeling. **D – F**. Examples of *Grm6-EGFP* retinas counterstained with CtBP2 (*red*). Single confocal planes. Scale bar 10 μm. **G – L**. Split channels of the same images as in *D – F*. *Circles* mark all EGFP ectopic terminals that typically contain at least one synaptic ribbon. *Arrowheads* point to *en passant* ribbons within smooth primary ON bipolar cell axons. A magenta-green version of this figure is available online as a supplemental figure.

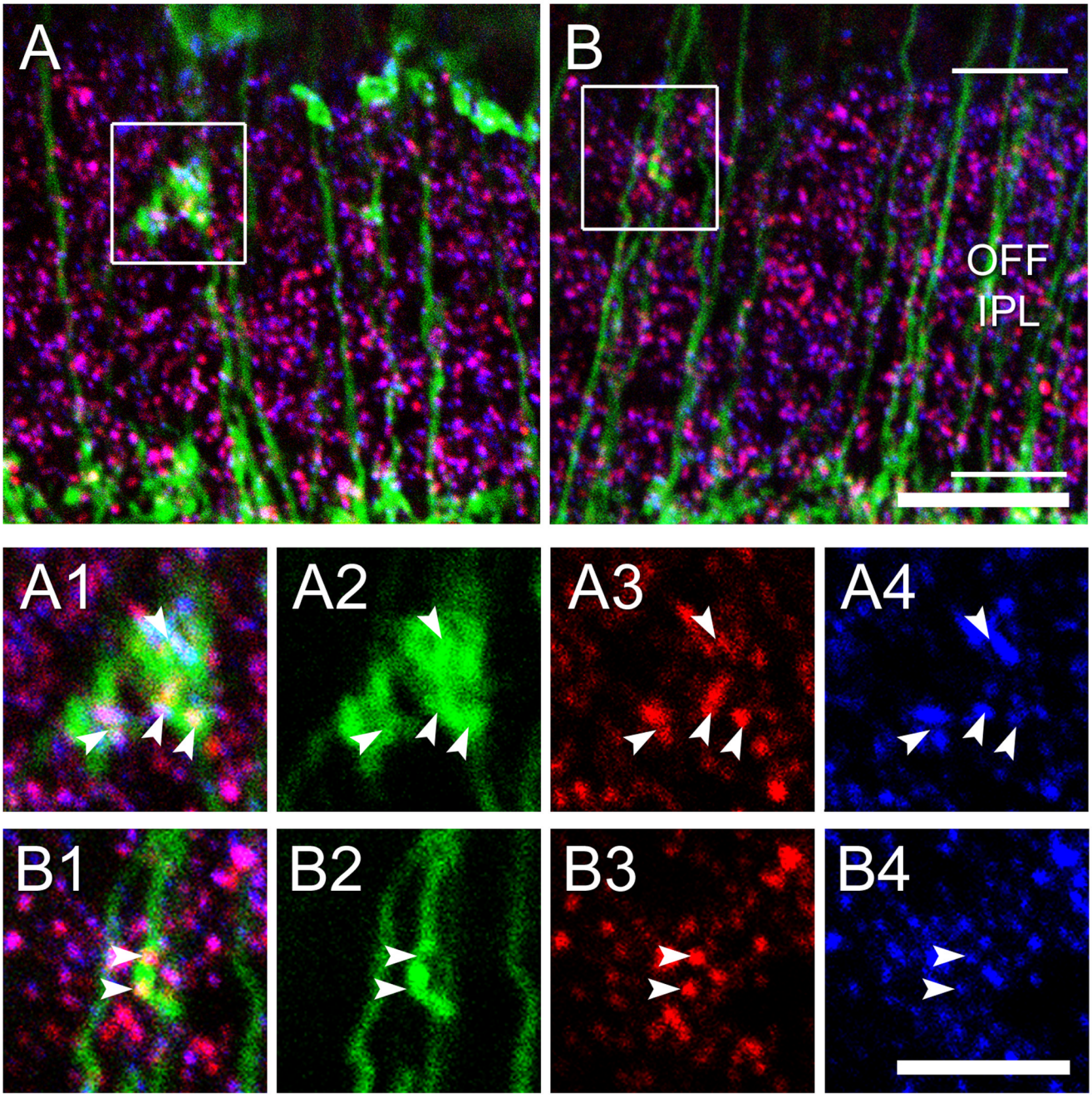

Figure 4. Ectopic ON bipolar cell ribbons in the OFF IPL are associated with postsynaptic glutamate receptors

A. Image of the OFF IPL in a vertical section of *Grm*6-*EGFP* retina immunostained for CtBP2 (*red*) and GluR3 (*blue*). Projection of confocal stack. Scale bar 10 μm. **B & C**. Single confocal planes at higher magnification of the insets in *A*. Both ectopic *en passant* ribbons (*B1 – 4*) and ribbons within ectopic terminals (*C1 – 4*) are associated with postsynaptic GluR3 puncta (*arrowheads*). Scale bar 5 μm.

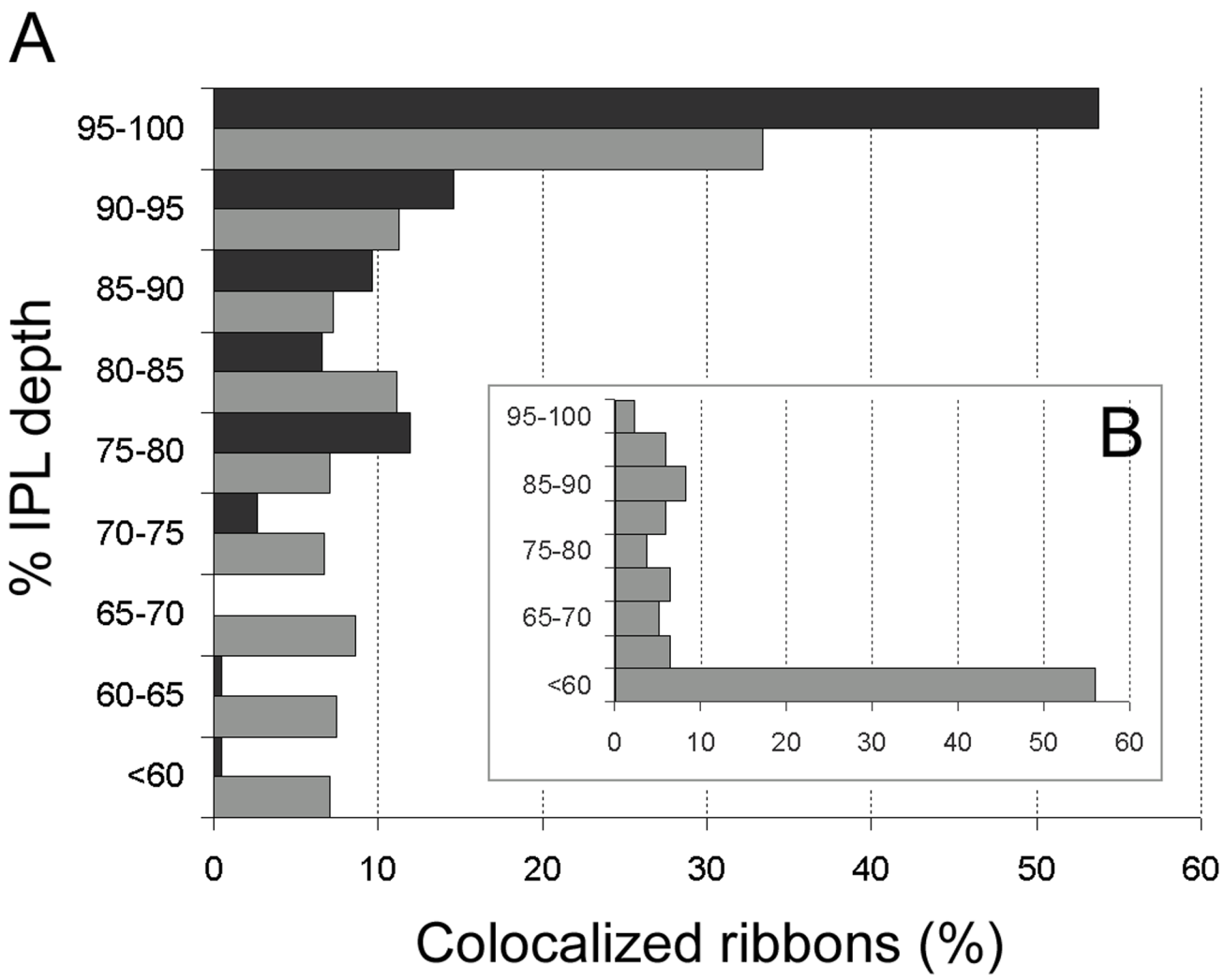

Figure 5. Ectopic ON bipolar synapses are concentrated near the IPL-INL border, where melanopsin and dopaminergic dendrites ramify

A. Comparative distribution throughout the OFF IPL of ribbons in ectopic terminals (*black bars*, *n* = 227) and in smooth axonal shafts (*en passant* synapses; *gray bars*, *n* = 495) of all ON bipolar cells in the *Grm*6-*EGFP* retina. Note the peak in density in the vicinity of the IPL-INL border (95–100% depth). **B**. Similar plot for *en passant* ribbons found only within rod bipolar cell axons (*n* = 218), as identified by PKCα immunoreactivity. Note the uniform distribution in depth and absence of a peak near the IPL-INL border.

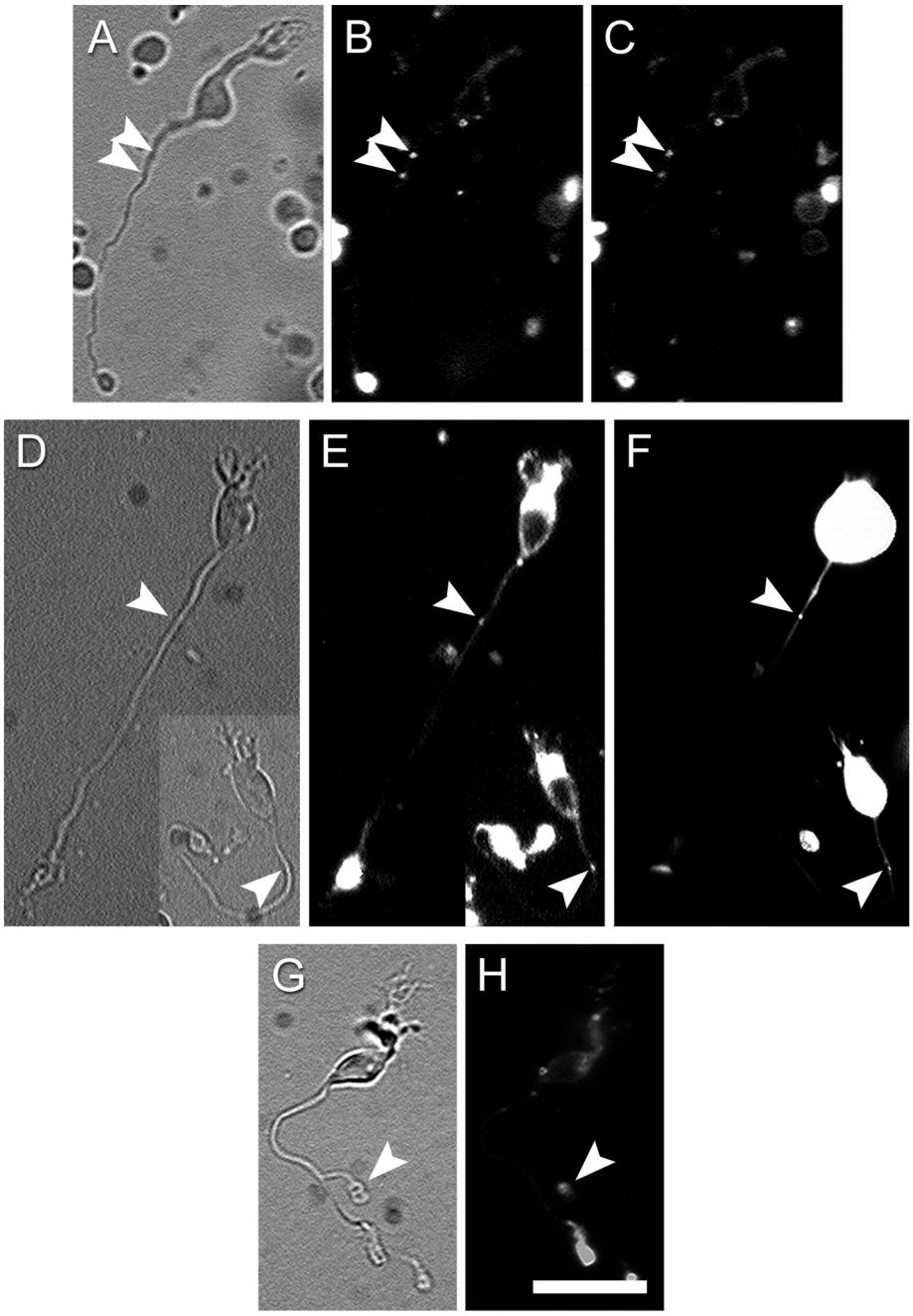

Figure 6. ON bipolar cells can uptake and release vesicles at ectopic synaptic sites

A – C. Depolarization triggered release of the styryl dye FM4-64 from a dissociated ON bipolar cell. *A:* Infrared image of the cell. *B:* FM4-64 staining in control Ringer with low K^+ and Ca^{2+}. *Arrowheads* indicate two puncta of FM4-64 staining in the proximal axon. *C:* FM4-64 staining of the same cell after 15-min incubation in a high-K^+, high-Ca^{2+} solution. Both puncta are noticeably dimmer when compared with those in the *B*. **D – F**. *En passant* vesicle cycling sites contain synaptic ribbons. In these two ON bipolar cells, *en passant* FM4-64 staining (*arrowheads* in *E*) colocalized with a RIBEYE-binding fluorescent peptide (*arrowheads* in *F*). **G – H**. ON bipolar cell with an ectopic axon terminal (*arrowhead* in *G*), which stained for FM4-64 (*arrowhead* in *H*). Scale bar = 20 μm.

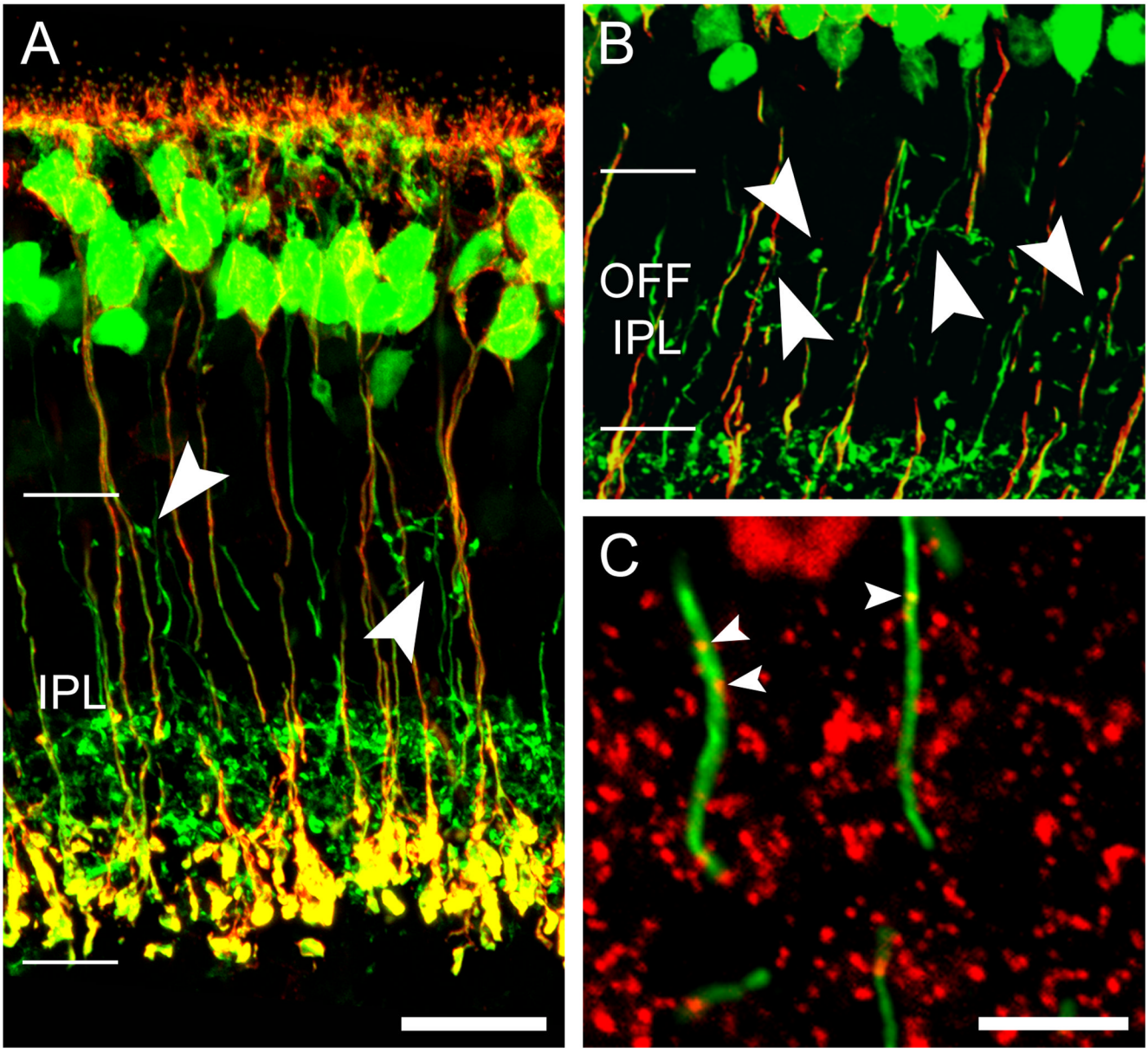

Figure 7. Rod bipolar cells do not appear to contribute to the ectopic ON bipolar output in the OFF IPL

A & B. Double immunofluorescence as seen in projected confocal stacks of vertical retinal sections showing all ON bipolar cells (*green*; *Grm6-EGFP* retina) and rod bipolar cells, marked by PKCα immunostaining (*red*). Ectopic ON bipolar cell terminals (*arrowheads*) never colocalize with the rod bipolar cell marker. Scale bar 20 μm. **C**. High magnification of a wild-type retina double stained against PKCα (*green*) and CtBP2 (*red*). *Arrowheads* point to *en passant* ribbons in the vicinity of the INL-IPL border. Scale bar 5 μm. A magenta-green version of this figure is available online as a supplemental figure.

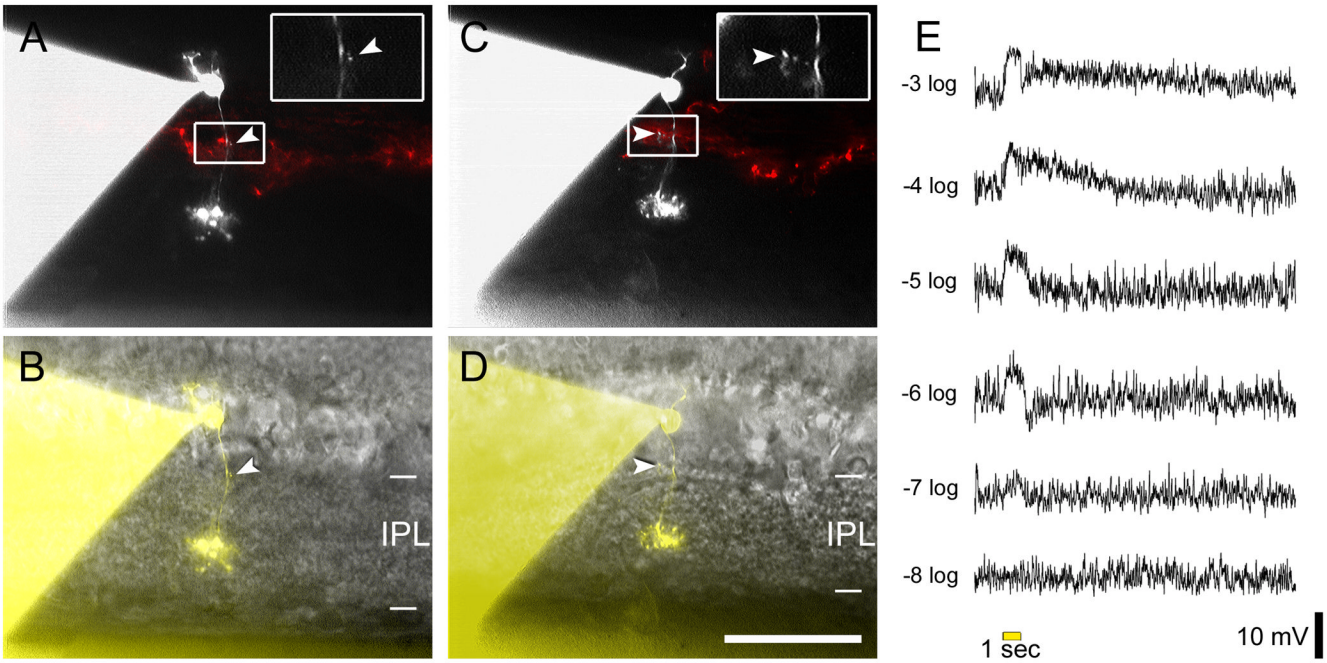

Figure 8. Type 6 bipolar cells possess ectopic axon terminals and depolarize to light

A & B. Intracellular HyLite488 fill of a bipolar cell with a small axonal protrusion near the INL-IPL border. *A* shows the HyLite488 staining in white and the RFP-labeled processes of DA cells in red. The *arrowhead* at the center highlights a small protrusion from the axon of this bipolar cell, which is shown at higher magnification in the *inset*. *B* shows the same bipolar cell in an infrared image of the retinal slice. The axonal protrusion (*arrowhead*) is near the outermost limit of the IPL. **C & D**. HyLite488 fill of another bipolar cell that has a longer axonal extension near the INL-IPL border. Scale bar 50 μm. **E**. Representative current-clamp light responses from a Type 8 bipolar cell that possessed an ectopic axon terminal in the distal IPL.

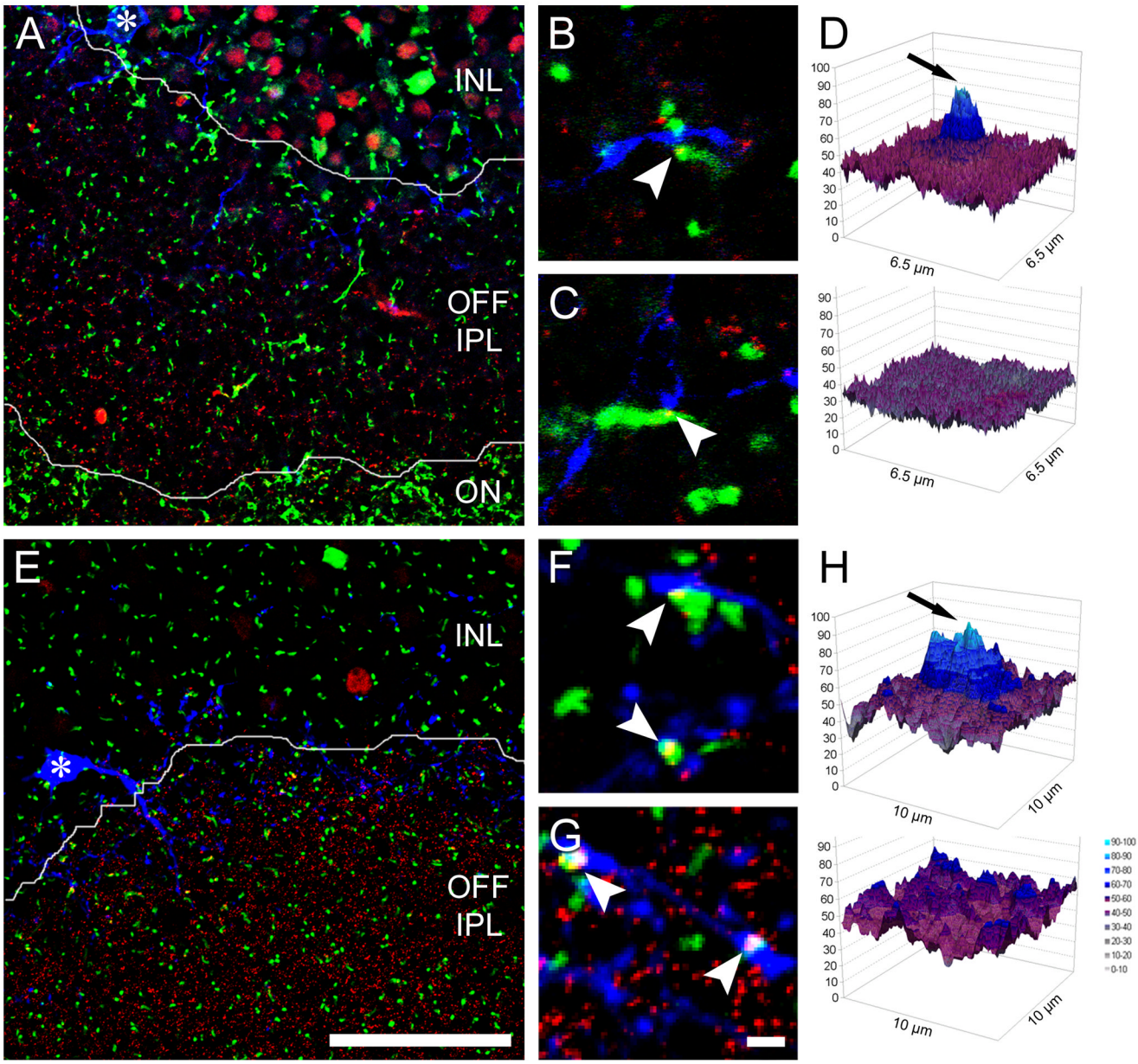

Figure 9. Ectopic ON bipolar cell ribbons are presynaptic to M1 ganglion cells and dopaminergic amacrine cells

A. Oblique retinal section of a *Grm6-EGFP* retina, double stained for the ribbon marker CtBP2 (*red*) and for melanopsin (*blue*). Single confocal plane. Borders between layers as indicated, *asterisk* marks soma of a displaced M1 cell. **B & C**. Two examples of ectopic ON bipolar cell ribbons in immediate apposition to a melanopsin-positive dendrite. **D**. *Top:* Pixel intensity plot of an averaged image showing the distribution of melanopsin immunoreactivity around ectopic bipolar ribbon synapses in the OFF sublayer (i.e., instances of EGFP-CtBP2 colocalization; average of 153 image samples). *Bottom:* Control plot showing that the correlation peak is abolished when the blue (melanopsin) channel is shifted along the isohypse defining the INL-IPL border. **E – H**. Images and analysis paralleling those in *A – D*, but showing the association of ectopic ON bipolar ribbons with

dendrites of DA cells, labeled with anti-TH antibodies (*blue*) (*H* is an average of 366 image samples). Scale bars 100 μm (*A*, *E*), 2 μm (*B*, *C*, *F*, *G*). Magenta-green versions of the micrographs in this figure are available online as a supplemental figure.